

BUREAU OF RECLAMATION  
HYDRAULIC LABORATORY**MASTER****FILE COPY**UNITED STATES  
DEPARTMENT OF THE INTERIOR  
BUREAU OF RECLAMATION

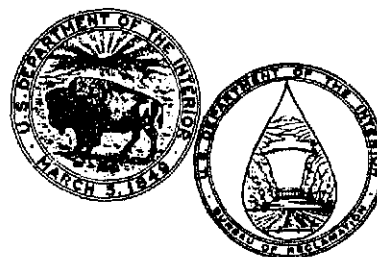
DO NOT REMOVE FROM THIS FILE

---

# SURGING IN A LABORATORY PIPELINE WITH STEADY INFLOW

## Report No. HYD-580

---

HYDRAULICS BRANCH  
DIVISION OF RESEARCHOFFICE OF CHIEF ENGINEER  
DENVER, COLORADO

---

SEPTEMBER 1967

The information contained in this report may not be used in any publication, advertising, or other promotion in such a manner as to constitute an endorsement by the United States Government or the Bureau of Reclamation, either explicit or implicit, of any material, product, device, or process that may be referred to in the report.

Where approximate or nominal English units are used to express a value or range of values, the converted metric units in parentheses are also approximate or nominal. Where precise English units are used, the converted metric units are expressed as equally significant values. A table of conversion factors--BRITISH TO METRIC UNITS OF MEASUREMENT--is provided at the end of this report.

Report No. HYD-580

**SURGING IN A LABORATORY PIPELINE  
WITH STEADY INFLOW**

by  
E. R. Holley

September 1967

HYDRAULICS BRANCH  
DIVISION OF RESEARCH

---

**UNITED STATES DEPARTMENT OF THE INTERIOR \* BUREAU OF RECLAMATION**  
Office of Chief Engineer . Denver, Colorado

#### ACKNOWLEDGMENTS

The author, who is Assistant Professor, Department of Civil Engineering, University of Illinois, performed this study while a Faculty Resident in Engineering Practice at the Office of Chief Engineer, Bureau of Reclamation, Denver, under a program of the Ford Foundation. The study was conducted under the supervision of Mr. W. E. Wagner, Head, Structures and Equipment Section. Mr. H. M. Martin is Chief of the Hydraulics Branch.

## CONTENTS

	<u>Page</u>
Abstract .....	iii
Notation .....	iv
Purpose .....	1
Conclusions .....	1
Applications .....	1
Introduction .....	2
Analytical Studies .....	3
Previous Work .....	3
Derivation of Differential Equation .....	3
Assumptions .....	3
Continuity and momentum .....	4
Discussion of the Solution .....	5
Experimental Program .....	7
Purpose .....	7
Description of Test Facility .....	7
Pipeline .....	7
Orifice calibration .....	8
Test Procedure .....	9
Surge measurement .....	9
Conditions investigated .....	9
Head Loss Determination .....	10
Experimental Results .....	11
Oscillograph recordings .....	11
Summary of results .....	11
Discussion of Results .....	12
Cause of surges .....	12
Comparison with analytical work .....	13
Comparison with unsteady inflow .....	16
Methods of surge control .....	16
References .....	19
Appendix .....	21

## FIGURES

<u>Figure</u>		<u>Page</u>
1	Possible types of check structures.....	41
2	Periodic inflow used in analysis of surges.....	42
3	Definition sketch for derivation of differ- ential equation .....	43
4	Magnitude of discharge surges .....	44
5	Asymmetrical surge resulting from variable damping.....	45
6	Experimental pipe system .....	46
7	Schematic diagram of experimental pipe system...	47
8	Calibration of orifice at Q1 .....	48
9	Surge tank .....	49
10	Head loss variations .....	50
11	Oscillograph record of surges, Run S69.....	51
12	Oscillograph record of surges, Run S19.....	52
13	Discharge and head surges with low head loss and without surge tank .....	53
14	Discharge and head surges with low head loss and with surge tank .....	54
15	Discharge and head surges with high head loss and with surge tank .....	55
16	Discharge and head surges with high head loss and without surge tank .....	56
17	Effects of head loss and surge tank on surges.....	57
18	Air entrainment and release for inflow of 0.03 cfs .....	58
19	Air entrapment and release for inflow of 0.13 cfs .....	59
20	Comparison of head surges at P6 for steady and unsteady inflows .....	60

#### ABSTRACT

Surges of head and discharge were studied experimentally in a laboratory pipe system having check structures spaced equally along the pipe. Surges developed when the downstream portion of the check structures did not flow full. The surges were initiated by the release of air entrained in the downstream leg of the check structures, and the surges were amplified as the flow passed through the successive pipe reaches. The experiments were made for various inflows steady at the upstream end of the system. Plots of surge magnitude vs. inflow rate showed two peaks. One peak apparently resulted from surges initiated by air release through the vent downstream of the check structures; the other peak originated from surges initiated by air release through the downstream leg of the check structure. The nonlinear momentum equation was integrated numerically to predict the growth of the discharge surge from one pipe reach to the next. The results were in good agreement with the experiments for different head loss conditions and for pipe reaches with and without surge tanks.

DESCRIPTORS-- \*pipelines/ \*surges/ hydraulic models/ laboratory tests/ surge tanks/ closed conduit flow/ fluid flow/ fluid mechanics/ computer programming/ hydraulics/ air entrainment/ check structures/ oscillation/ \*water pipes/ momentum  
IDENTIFIERS-- \*pipeline surges/ Runge-Kutta method/ surge waves

## NOTATION

<u>Symbol</u>	<u>Definition</u>	<u>Dimensions</u>
A	Cross sectional area of pipe	$L^2$
B	Overall head loss coefficient	
F	Cross sectional area of vertical pipe; force	$L^2$ F
$H_L$	Head loss associated with boundary forces	L
L	Length of pipe	L
Q	Discharge	$L^3/T$
$Q_m$	Amplitude of inflow oscillation	$L^3/T$
$Q_s$	Average inflow	$L^3/T$
$Q_r$	$Q_s/Q_m$	
$Q'$	$Q/Q_m$	
R	Damping coefficient	
T	Period of oscillation	T
$T_o$	Period of inflow oscillation	T
$T_n$	Undamped natural period of oscillation	T
$T_r$	$T_o/T_n$	
V	Velocity (Q/A)	L/T
g	Gravitational acceleration	$L/T^2$
t	Time	T
t'	$t/T_o$	
Y	Water surface elevation in vertical leg of pipe	L
$\gamma$	Specific weight of fluid	F/L <sup>3</sup>
$\rho$	Density of fluid ( $\gamma/g$ )	M/L <sup>3</sup>

## PURPOSE

Analytical and experimental studies were made to investigate the type and magnitude of surges which can develop when there is steady inflow into a pipe system containing a series of check structures. Methods of surge control were also investigated.

## CONCLUSIONS

Surges of head and discharge can develop for steady inflow into a pipe system which contains a series of check structures. Small surges existed in the upstream part of the pipe system and these surges were amplified as the flow passed through successive pipe reaches. In this study the release of air which was entrained in the downstream part of the check structures seemed to be the disturbance which initiated the surges.

An analysis has been developed and has been used successfully to predict the change in surge magnitude from one pipe reach to the next both when the downstream reach had no surge tank and when it included a surge tank.

It was found both analytically and experimentally that the magnitude of surging was reduced by the use of a surge tank. However, a tank did not completely remove the surging and the remaining surge was amplified again as the flow passed through the reaches downstream of the tank.

## APPLICATIONS

There are many types of flow disturbances which can start surging. These disturbances never can be completely eliminated. It is more practicable to seek means of controlling surge magnitude rather than trying to remove all the possible causes of surging.

The maximum amount of amplification of flow disturbances occurs when the natural period of oscillation for a pipe reach is the same as the period of an inflow disturbance. This undesirable situation often occurs when the pipe reaches between successive check structures are identical and consequently have the same natural periods of oscillation. Generally, any modifications that will change the natural frequency of oscillation in successive pipe reaches will reduce the amount of surge amplification. The most benefit is obtained if the natural period of a pipe reach is greater than 1.4 times the period of the inflow oscillation. Under this condition, the incoming flow disturbance will be damped rather than amplified. The natural period may be increased by increasing the length of

pipe in a reach or by including a surge tank in the reach. An analysis is given in the report to estimate the amount of reduction in surge amplification which would result from a given change in a pipe reach.

## INTRODUCTION

Water delivery systems are tending more and more to be systems of closed conduits rather than open channels. In pipe systems, there is generally a choice of having the control valve either at the upstream end or at the downstream end. If the control valve is placed at the downstream end of the pipeline, then the design pressure for the pipe must be derived from the elevation difference along the pipe to account for the hydrostatic condition when the valve is closed. When the drop in elevation along the pipe is large, the design pressure for the pipe may become prohibitive. On the other hand, if an upstream control valve is used, it may be possible to use a lower design pressure.

When upstream control is used, check structures must be spaced along the pipe. Three possible types of check structures are shown in Figure 1. No doubt other configurations could also be used. Whatever the configuration, the structure must (1) provide an overflow point high enough in elevation to keep the pipe from draining when there is no inflow, (2) have a great enough total height so that the structure does not overflow for the design discharge or, in other words, enough height so that the hydraulic gradient always passes below the top of the structure, and (3) provide an air source to keep negative pressures from developing when the discharge is less than the design value.

Usually the check structures are designed so that the hydraulic gradient is above the crest of the check for the design discharge (Figure 1). For smaller discharges, water spills into the downstream portion of the structure. Thus for discharges less than the design value, the check structures effectively divide the pipe into separate reaches. (The term "reach" is used here to refer to the length of pipe between two check structures.) It is possible for the flow in the various reaches to interact in a manner to develop surges of discharge and piezometric head. Surging may be caused by variation of the inflow rate. This type of surging is being studied by the Canals Branch of the Bureau of Reclamation in connection with their design of the Canadian River Aqueduct in the northwestern part of Texas (Reference 1).

Surging may also develop for a steady inflow if a source of disturbance is present. These disturbances may be initiated by the escape

of air which is entrained in the downstream portion of the check structures, by pressure drop due to wind blowing over a vent, or by anything else that causes a momentary unsteadiness in the flow. Thus, analytical and experimental work was undertaken in the Hydraulics Branch of the Bureau of Reclamation to study surges which develop when the inflow is steady.

## ANALYTICAL STUDIES

### Previous Work

Glover (Reference 2) has previously reported some analytical work on pipeline surges. Part of his work applied the analysis of forced vibrations (Reference 3, page 56) to the inertial surges which develop in a single reach of pipe in response to a periodic inflow. The inflow which he considered may be written as

$$Q_{in} = Q_m \sin(2\pi t/T_o) + Q_s \quad 1$$

where  $Q_m$  is the amplitude of the inflow oscillation,  $t$  is time,  $T_o$  is the period of the inflow, and  $Q_s$  is the average inflow. He assumed that  $Q_s$  was much greater than  $Q_m$  and thus that the damping could be taken as linear, i. e., that the head loss in the pipe varied as the first power of the velocity. For these conditions, he presented amplification factors in Figure 10 and in Equation 17 of Reference 2. The amplification factor was defined as the ratio of the maximum flow in the pipe to  $Q_m$ .

### Derivation of Differential Equation

Assumptions. --The present analysis extended Glover's work by removing the restriction that  $Q_s$  must be much greater than  $Q_m$  and by considering square-law damping, i. e., taking the head loss variations as proportional to the velocity squared. The dimensionless inflow was written as

$$Q'_{in} = \sin(2\pi t/T_o) + Q_r \quad \text{if } \sin(2\pi t/T_o) + Q_r \geq 0 \quad 2a$$

$$Q'_{in} = 0 \quad \text{if } \sin(2\pi t/T_o) + Q_r < 0 \quad 2b$$

where  $Q'_{in} = Q_{in}/Q_m$  and  $Q_r = Q_s/Q_m$ . Equation 2b was used to assure that the analysis never took  $Q'_{in}$  as negative. If  $Q_s$  was greater than or equal to  $Q_m$  ( $Q_r \geq 1$ ), then  $Q'_{in}$  of Equation 2a was never negative and there was no need to use Equation 2b. One period of Equation 2 is plotted in Figure 2 for both  $Q_s > Q_m$  ( $Q_r > 1$ ) and  $Q_s < Q_m$  ( $Q_r < 1$ ).

The head loss  $H_L$  was taken as being proportional to the square of the velocity according to the equation

$$H_L = B \frac{V|V|}{2g} \quad 3$$

B is an overall loss coefficient. The absolute value of the velocity was needed to preserve the correct sign for  $H_L$  if the flow reversed in the pipe.

Continuity and momentum. --The physical situation which was analyzed is shown in Figure 3. Assuming the water to be incompressible, continuity in the upstream vertical leg required that

$$\frac{dy}{dt} = \frac{Q_{in} - Q}{F} \quad 4$$

where F was the horizontal area available for storage of water as the water surface rose and fell. Equation 4 assumed that water never overflowed the upstream leg of the pipe. Also, F was taken as a constant in the analysis, thus effectively assuming that the water surface never fell into the horizontal pipe.

It was assumed that the rate of change of momentum of water in the vertical legs was small compared to that in the horizontal pipe. The validity of this assumption was born out by previous work (Reference 2). Under the stated conditions, the momentum relation for the horizontal pipe was developed as follows:

$$\Sigma \text{ external forces} = \text{mass} \times \text{acceleration}$$

$$\gamma y A - \Sigma F_b = \rho A L \frac{dV}{dt}$$

$$y - \frac{\Sigma F_b}{\gamma A} = \frac{L}{g} \frac{dQ}{dt}$$

where  $\gamma$  is the specific weight of the water,  $\Sigma F_b$  is the sum of the boundary forces acting on the water in the horizontal pipe, and V is the velocity of flow in the pipe.  $H_L$  was defined as

$$H_L = \frac{\Sigma F_b}{\gamma A}$$

so that  $H_L$  was only that part of the head loss associated with boundary forces and did not include head loss due to the decay of turbulence generated by the inflow. With this definition of  $H_L$ , the momentum relation becomes

$$y - H_L = \frac{L}{g} \frac{dQ}{dt} \quad 5$$

Equations 4 and 5 can be combined to eliminate  $y$  by differentiating Equation 5 with respect to  $t$ . Replacing  $H_L$  from Equation 3 and writing the resulting equation in dimensionless form, one obtains

$$\frac{d^2 Q'}{dt'^2} = -4\pi R T_r |Q'| \frac{dQ'}{dt} - 4\pi^2 T_r^2 Q' + 4\pi^2 T_r^2 Q'_{in} \quad 6$$

where  $Q' = Q/Q_m$

$$t' = t/T_0$$

$$T_r = T_0/T_n$$

$$T_n = 2\pi \sqrt{FL/gA}$$

$$R = \frac{B Q_m}{2AL} \sqrt{\frac{FL}{gA}}$$

To obtain Equation 6,  $d|Q'|/dt$  was replaced by  $(\text{sign } Q') dQ'/dt$  and then  $(\text{sign } Q') \cdot Q'$  was replaced by  $|Q'|$ .  $T_n$  is the undamped natural period of oscillation of the pipe (Reference 2 or 4).  $R$  is called a damping coefficient since  $R$  is proportional to  $B$ , which is a measure of the head loss (friction) in the pipe.

#### Discussion of the Solution

The solution of Equation 6 gives  $Q'$  as a function of  $t'$ . As time increases, this solution becomes periodic with period  $T_0$ . That is, when the initial transients die out, the flow in the pipe oscillates with the same period as the inflow. The periodic part of the solution depends on the three dimensionless parameters  $Q_m$ ,  $R$ , and  $T_r$ . The length of time required for the pipe flow to become periodic also depends on these three parameters and on the initial conditions used for the solution of Equation 6.

Equations 4 and 5 could also be combined so as to eliminate  $Q'$  instead of  $y$ . Then an equation similar to Equation 6 would be

obtained but with  $y$  as the dependent variable and with a fourth dimensionless parameter in addition to  $Q_r$ ,  $R$ , and  $T_r$ .

Since Equation 6 is nonlinear, it was solved numerically using the Runge-Kutta technique (Reference 5, page 358). The FORTRAN computer program used for the solution is listed in Appendix A. The program was written so that any type of damping and any type of inflow could be used by inserting the proper statements in a function subprogram. The accuracy of the program was verified for the case of linear damping by comparing the numerical results with the analytical results presented by Glover (Reference 2). The results of the program were also checked to see that the average pipe flow was equal to the average inflow, that the pipe flow was symmetrical with respect to zero for  $Q_r = 0$ , and that the ultimate periodic flow was independent of the initial conditions used for the solution.

From the numerical computations, the maximum and minimum values of  $Q'$  are plotted in Figure 4 for  $Q_r = 1$  and  $Q_r = 2$ . In each case, a range of values for  $T_r$  and  $R$  is covered. The numerical solution did not converge for  $R = 0$ . The limiting curves for the hypothetical case of  $R = 0$  were obtained analytically from the particular integral ( $Q'_p$ ) of Equation 6 with  $R = 0$ . As Glover points out (Reference 2), the particular integral represents the conditions after the initial oscillations have died out. It can be verified by substitution that a particular integral is given by

$$Q'_p = \frac{T_r^2}{T_r^2 - 1} \sin 2\pi t' + Q_r$$

so that the maximum and minimum values of  $Q'$  are given by

$$Q'_{\max, \min} = Q_r \pm \frac{T_r^2}{T_r^2 - 1} \quad 7$$

For  $T_r < 1$ , the minus sign gives  $Q'_{\max}$  and the plus sign gives  $Q'_{\min}$ . For  $T_r > 1$ , the opposite is true.

Referring to Figure 4, it can be seen that as  $T_r$  approaches zero, the flow in the pipe approaches a steady state (no oscillation and  $Q' = Q_r$  or  $Q = Q_s$ ) regardless of the value of  $R$ . A very long pipe where  $T_n$  was much greater than  $T_o$  would be one condition that would give  $T_r$  approaching zero. Another method of obtaining a large  $T_n$  would be to have the area ( $F$ ) of the upstream leg much larger than the area ( $A$ ) of the pipe. On the other hand, as  $T_r$

gets larger, the oscillations in the pipe flow become equal in magnitude to the inflow oscillations. This condition might correspond to a very short pipe where  $T_n$  was much smaller than  $T_0$ .

For  $R > 0$  and  $Q_T > 0$ , the pipe flow ( $Q'$ ) is not symmetrical with respect to  $Q_T$  even though the flow is periodic. This asymmetry results from the damping which is proportional to the velocity. Thus, the discharges near zero receive less damping than the discharges farther from zero. The asymmetry for a typical case is shown in Figure 5, which also shows schematically the variation of damping and amplification as the discharge varies. The asymmetry is also evident from the curves in Figure 4 in that  $Q'_{min}$  tends to deviate more from  $Q_T$  than  $Q'_{max}$  does, i. e.,

$$|Q'_{min} - Q_T| > |Q'_{max} - Q_T|$$

The evidence of greater damping of higher flows may also be seen by comparing the curves in Figure 4 for  $Q_T = 1$  with those for  $Q_T = 2$ . For  $Q_T = 2$  the dimensionless inflows vary from 1 to 3 while for  $Q_T = 1$ , the inflows vary from 0 to 2. Thus, for a given  $R$ , the inflows are greater on the average and are, therefore, more highly damped for the higher  $Q_T$ . This shows up in the fact that  $Q'_{max}$  is always less than  $Q_T + 1$  for  $R = 0.3$  if  $Q_T = 2$ , while a value of about  $R = 0.6$  is required for  $Q'_{max}$  to be less than  $Q_T + 1$  if  $Q_T = 1$ .

## EXPERIMENTAL PROGRAM

### Purpose

The purpose of the experimental program was (1) to investigate the magnitude and type of both discharge surges and head surges which occur with steady inflow into the laboratory pipeline, (2) to seek an explanation for the surging, (3) to check the validity of the analytical work described above, and (4) to seek possible means of surge reduction.

### Description of Test Facility

Pipeline. --The general layout of the pipeline system which was used for these surge studies is shown in Figures 6 and 7. This pipeline was originally built in the Hydraulics Laboratory of the Bureau of Reclamation for studies requested by the Canals Branch.

The primary features of the pipeline were the pipe checks spaced along the pipelines. The purpose of the pipe checks was discussed

in the introduction. A study of the hydraulics of the pipe checks has been previously reported (Reference 6).

The majority of the pipe was 4-inch (10.2-cm) outside-diameter by 3.9-inch (9.8-cm) inside-diameter aluminum. In the pipe checks, the top 180° bend and the downstream leg were made of 3.75-inch (9.52-cm) inside-diameter transparent plastic. There were deposits (apparently aluminum oxide) throughout the aluminum pipe. A height of deposit of 1/16 to 1/8 inch (1/6 to 1/3 cm) and a lateral dimension of 1/4 inch (3/4 cm) were not uncommon. The spacing between deposits was of the order of 2 to 3 inches (5 to 10 cm).

Downstream of each check stand, the pipeline had, in order, (1) a 2-inch (5.1-cm) diameter vertical pipe to serve as a release vent for air entrained in the downstream leg of the pipe check, (2) a piezometer tap at the same elevation as the centerline of the pipe, (3) a 2.500-inch (6.350-cm) diameter orifice with pressure taps, and (4) a sliding gate to allow regulation of the amount of head lost between pipe checks.

Orifice calibration. --A calibration of the first orifice (Q1) at the upstream end of the pipe is shown in Figure 8. The discharge coefficient for this orifice, which was calibrated in place, was 0.667 giving a discharge equation of

$$Q \text{ (cfs)} = 0.183 \sqrt{\Delta H \text{ (ft)}} \quad 8$$

No calibration was done for reverse flow through the orifice. The calibration (Equation 8) was found to be valid for orifices Q5 and Q6 also. The discharge coefficient for orifices Q4 and Q7 was 2 percent lower (0.654) giving a discharge equation of

$$Q \text{ (cfs)} = 0.179 \sqrt{\Delta H \text{ (ft)}} \quad 9$$

for these two orifices. The orifices Q2 and Q3 were not calibrated and were not used in this study.

The orifices were calibrated for steady flow and then used to measure unsteady flow. It is felt that the unsteadiness did not introduce appreciable error because of the relatively slow acceleration of the flow (Reference 7) and because the head drop was sensed with an electronic (variable reluctance) pressure transducer and recorded on a strip oscillograph. The period of oscillation was of the order of 17 seconds.

## Test Procedure

Surge measurement. --The regulating valve downstream of the head box was set in a fixed position thus establishing a steady inflow into the pipeline. The inflow rate was measured at the orifice Q1. When the check stands were not flowing full, surges generally developed in the pipeline. The surging of head and discharge were recorded by pressure transducers and a multi-channel oscillograph.

Because of the noise which developed in the electronic measuring system, a 1-second averaging time was usually imposed on the output of the pressure transducers before this output was recorded. The noise was probably due to physical vibration of the transducers, but pressure surges in the tubes leading to the transducers may have been a contributing factor. The amplitude of the noise was too great to have been due to turbulent pressure fluctuations in the pipe. Since the period of the surging was about 17 seconds, it is felt that the 1-second averaging did not appreciably affect the results.

Conditions investigated. --Data were taken at the various piezometer stations and discharge stations for four hydraulic conditions:

- (1) Sliding gates completely open (called "low head loss")--  
Runs S1-S22
- (2) Low head loss and an 8-inch-diameter surge tank downstream of pipe Check 5--Runs S23-S47 and S102-S110
- (3) Sliding gates partially closed (called "high head loss")  
and same surge tank as Condition No. 2--Runs S48-S69  
and S93-S101
- (4) High head loss and no surge tank--Runs S68A-S92

The surge tank was installed by replacing the 2-inch (5.1-cm) air release vent pipe downstream on Check 5 with an 8-inch (20.3-cm) pipe as shown in Figure 9. Thus, there was a 2-inch (5.1-cm) diameter nipple about 1 inch (2.5 cm) long between the 4-inch (10.2-cm) pipe and the 8-inch (20.3-cm) surge tank.

For the high head loss condition, the settings of the slide gates were adjusted by trial until the piezometric head stood 0.7 foot (18 cm) above the invert of the top of each pipe check for an opening of 5.47 inches (13.9 cm) in the control valve. This setting gave a discharge of 0.153 cfs (4330 cc/sec).

### Head Loss Determination

When the pipe checks did not flow full, the total loss of head between any two checks was always equal to the difference in elevation between the top inverts (overflow points) in the checks. Part of this head loss was due to the decay of turbulence generated as the water spilled into the downstream leg of the check.

As mentioned previously in the section of Analytical Studies, the head loss which is significant as a damping agent in surge analysis is only the loss due to the boundary forces. This loss was determined in two ways: (1) by measuring the total loss between any two checks flowing full and (2) by measuring the loss between the piezometer tap downstream of one check and the top invert of the next check. For the first method with the checks flowing full, there was no head loss due to water spilling into the downstream leg of the checks. Thus, all of the head loss was due to boundary forces. For the second method, the piezometer was 90 inches (229 cm) downstream of the pipe check. Thus, the head loss measured by this method excluded the loss due to water spilling over the pipe check. For this method, the loss was measured in only the first two pipe reaches because of the surges which developed in the lower reaches.

The results of the head loss measurements are shown in Figure 10. In order to fit the data, two straight lines were used on log-log paper. For the low head loss, the equations used for  $H_L$  were

$$H_L = 30 Q^{1.5} \text{ for } Q < 0.10 \text{ cfs} \quad 10a$$

$$H_L = 45 Q^{1.65} \text{ for } Q > 0.10 \text{ cfs} \quad 10b$$

while for the high head loss, the corresponding equations were

$$H_L = 37 Q^{1.5} \text{ for } Q < 0.10 \text{ cfs} \quad 11a$$

$$H_L = 55 Q^{1.65} \text{ for } Q > 0.10 \text{ cfs} \quad 11b$$

where  $H_L$  is in ft and  $Q$  is in cfs.

$H_L$  for the higher head loss is 1.23 times that for the lower head loss condition. Notice from Figure 10 that the head loss data did not extend below  $Q = 0.03$  cfs (850 cc/sec) but that Equations 10a and 11a were taken as applying for  $Q < 0.03$  cfs (850 cc/sec). In this range,  $H_L$  was probably higher than indicated by the equations.

For high enough Reynolds numbers in hydraulically rough pipes,  $H_L$  is proportional to  $Q^2$ . However, since the pipe Reynolds number used in determining  $H_L$  varied only from about  $10^4$  to  $6 \times 10^4$ ,

it should not be surprising that  $H_L$  was proportional to  $Q$  to a power less than two.

### Experimental Results

Oscillograph recordings. --Typical oscillograph recordings for part of two runs are shown in Figures 11 and 12. From the recordings, the following observations were made:

(1) For a given measurement station and a given steady inflow the amplitude of the surges varied in time. The surges sometimes almost died out and then began again. This fact indicated that the surges were caused by some flow disturbance and not from the unsteadiness which occurred while the inflow was being established. A given large or small surge generally traveled down the pipe and could be detected at successive measurement stations.

(2) For the lower inflow rates (approximately 0 to 0.10 cfs (2,800 cc/sec)), the surges occurred with an essentially constant frequency. The shape of the surges was not truly sinusoidal, but generally had a sharper crest and a flatter trough than a sine wave.

(3) For the higher inflow rates (about 0.10 cfs (2,800 cc/sec) until the pipe checks began to flow full), the interval of occurrence of the surges was irregular and the shape generally did not even approximate a sine wave. Rather, the negative part of the surge was always larger in amplitude than the positive part of the surge.

Summary of results. --For each inflow rate, oscillograph records of the type discussed above were taken for at least 7 or 8 minutes. From each of these records, the largest surge was selected and the maximum and minimum points on the surge were plotted on summary graphs for a given hydraulic condition and a given measurement station. These summary graphs are presented in Figures 13 to 16. Some of the data which indicated an average discharge greatly different from the true average discharge were not included on the summary graphs. From the graphs, the following observations were made:

(1) The data points do not fall on well-defined curves. The scatter of the data points no doubt resulted from factors already mentioned, namely that the amplitude of the surges varied with time and that about 7 or 8 minutes of record was taken for each station. Due to the varying amplitude, the maximum surge which occurred in the period of record was

evidently not always the same. Thus, it seems that the envelopes sketched on the summary graphs are more significant than the scatter of the individual data points. The envelopes represent approximately the extremes of the surges which occurred during the testing program.

(2) On all of the summary graphs which cover the full range of inflows, there are two peaks in the surge envelope. The first peak occurred for the type of surges mentioned in Comment No. 2 in the paragraph on Oscillograph Recordings, and the second peak occurred for the type of surge mentioned in Comment No. 3.

(3) The effect of the 23 percent change in the head loss condition (Equations 10 and 11) can be seen by comparing the graphs for the same measurement station but with the different loss condition. For convenience, a comparison is presented in Figure 17A. As would be expected, the surges were somewhat smaller for the higher head loss. Also, the surges stopped altogether at a lower discharge for the high head loss than for the low head loss. This was due to the fact that the downstream leg of the pipe checks began to flow full at a lower discharge for the higher  $H_L$ .

(4) Using Figure 14A, B, and C as an example, it is seen that the surge tank caused the surge in Reach 5 to be less than the incoming surge from Reach 4. However, downstream of Reach 5, the surge was amplified again. The effect of the surge tank on reducing the surge at a given point also is shown in Figure 17B, which compares the discharge surge at Q6 with and without the surge tank in Reach 5.

### Discussion of Results

Cause of surges. --For these experiments which were made for a steady inflow, the storage and release of entrapped air seems to have been the source of initiating the surges. Water falling into the downstream leg of the pipe checks entrained air, and some of this air was carried into the horizontal pipe where it collected into large bubbles along the top of the pipe. These bubbles were released either by traveling downstream and escaping through the air release vent pipe or by traveling upstream and out through the pipe check. The released air was replaced by water, thus a temporary unsteadiness in the flow was created and some unbalanced momentum was fed into the flow. A small oscillation resulted from the unbalanced momentum, and further releases of air then took place in phase with the oscillations which existed in the pipe.

The amplitude of these oscillations or surges ordinarily was not large and would have been of minor significance if another factor had not been involved. The equal spacing of the pipe checks provided a succession of pipe reaches with nearly identical natural periods of oscillation. Thus, the small oscillations which originated in the upstream reach were amplified into sizable surges as the flow passed through successive pipe reaches. (See discussion in Reference 2 also.)

It is felt that the two peaks in the surge envelope can be explained by two different modes of air entrapment and release which were observed to take place. Refer to Figure 13A for an example of the surge envelope and so that specific numbers may be used in the following discussion. For inflows from 0 to about 0.10 cfs (2,800 cc/sec), the entrained air which was carried downstream by the flow was released through the 2-inch (5.1-cm) air release vent and surges resulted as discussed above (see Figure 18). As the inflow increased above 0.03 cfs (850 cc/sec), the reduction in the magnitude of the surges was probably due to the increased resistance or damping associated with the higher flow rates. For inflows above 0.10 cfs (2,800 cc/sec), the flow began to show a significant separation as it passed through the first 45 degree bend at the bottom of the pipe check. Some of the entrained air collected in this separation zone, and when the volume of air became great enough, the large bubble passed back up through the downstream leg of the pipe check, (see Figure 19). In this manner, a larger bubble could collect and escape through the check than through the 2-inch vent. Thus, a larger flow disturbance occurred and surging increased again. The surging ceased for an inflow of about 0.15 cfs (4,300 cc/sec) because the pipe checks were essentially flowing full at this discharge. It has already been observed that the character of the surges for inflows above 0.10 cfs (2,800 cc/sec) were different from those for lower inflows.

Comparison with analytical work. --From the experimental work, the surges which occurred in one reach of pipe were taken as the inflow variations for prediction of the surges in the next pipe reach. Of course, when a negative flow occurred in one reach, the inflow to the next reach was zero rather than negative. This situation was accounted for in the analytical inflow of Equation 2 and Figure 2. As previously mentioned, the shape of the experimental surges was not truly sinusoidal.

It is possible that a negative inflow could occur in a reach if the surge in that reach became great enough that water flowed back over the overflow point in the check at the upstream end of the reach. This possibility was not considered in the analysis.

In order to predict the surges in the second reach, values were needed for  $Q_s$ ,  $Q_m$ , and  $Q_r$  to characterize the inflow and for  $R$  and  $T_r$  to characterize the pipe. The values used for  $Q_s$ ,  $Q_m$ , and  $Q_r$  are indicated on the summary graphs of the surges (Figures 13A, 14A, 14B, 15A, 15B, and 16A). For conditions where the negative part of the surge was much greater than the positive part (e. g., inflow of 0.127 cfs (3,600 cc/sec) on Figure 13A),  $Q_s$  was taken as the average of the maximum and minimum values of the discharge rather than as the actual average discharge.

The damping coefficient  $R$  was calculated according to the definition following Equation 6. The analysis assumed that the damping followed a square law while the head loss actually varied as some power less than two. This condition was taken into account by assuming that the head loss coefficient varied with discharge. Using Equations 3, 10, and 11 and using  $Q_s$  as the basis for calculating  $B$ , one may show for the low head loss condition that

$$B = 30(2gA^2)/Q_s^{0.50} \quad \text{for } Q_s < 0.10 \text{ cfs} \quad 12$$

$$B = 45(2gA^2)/Q_s^{0.35} \quad \text{for } Q_s > 0.10 \text{ cfs}$$

and

$$R = 1.07 \frac{Q_s^{0.50}}{Q_r} \sqrt{\frac{F}{A}} \quad \text{for } Q_s < 0.10 \text{ cfs} \quad 13$$

$$R = 1.60 \frac{Q_s^{0.65}}{Q_r} \sqrt{\frac{F}{A}} \quad \text{for } Q_s > 0.10 \text{ cfs}$$

and for the high head loss condition that

$$B = 37(2gA^2)/Q_s^{0.50} \quad \text{for } Q_s < 0.10 \text{ cfs} \quad 14$$

$$B = 55(2gA^2)/Q_s^{0.35} \quad \text{for } Q_s > 0.10 \text{ cfs}$$

and

$$R = 1.32 \frac{Q_s^{0.50}}{Q_r} \sqrt{\frac{F}{A}} \quad \text{for } Q_s < 0.10 \text{ cfs} \quad 15$$

$$R = 1.96 \frac{Q_s^{0.65}}{Q_r} \sqrt{\frac{F}{A}} \quad \text{for } Q_s > 0.10 \text{ cfs}$$

In these equations,  $Q_s$  must be in cfs. In calculating R, the pipe area (A) of 0.0830 ft<sup>2</sup> (77.1 cm<sup>2</sup>) and the total length (L) of 175.4 ft (53.5 m) between pipe checks has been used. The factor  $\sqrt{F/A}$  was unity for the pipe reaches without a surge tank. With an 8-inch (20.3-cm) diameter surge tank,  $\sqrt{F/A}$  was equal to  $\sqrt{5}$  since the area F included both the area of the downstream leg of pipe check and the surge tank area which was four times that of the pipe.

When no surge tank was used,  $T_r$  was taken as unity since the frequency of the inflow variations was about the same as the natural frequency of the pipe reaches. For predicting surges in a pipe reach with a surge tank, it was assumed that the period of the inflow variations was equal to the natural period of the pipe reaches upstream which did not have surge tanks (Subscript 1). The natural period of the reach with the surge tank (Subscript 2) was assumed to be given by the definition of  $T_n$  following Equation 6. Thus

$$T_r = \frac{T_o}{T_n} = \frac{2\pi\sqrt{\frac{L_1}{g}}}{2\pi\sqrt{\frac{L_2}{g} \frac{F_2}{A_2}}} = \sqrt{\frac{A_2}{F_2}} = \frac{1}{\sqrt{5}} = 0.45$$

since  $L_1 = L_2$  and the area F includes both the area of the downstream leg of the pipe check and the area of the surge tank. For  $T_r = 0.45$ , the predicted surges are not very sensitive to the value of R as long as R is less than about 0.5, (see Figure 4).

The predicted surges are shown in comparison with the data in Figures 13A, 13B, 14B, 14C, 15B, 15C, 16A, and 16B. Since the scope of the analytical curves presented in Figure 4 is rather limited, the predicted surges were obtained by the numerical solution of the differential equation (Equation 6) for each condition indicated on the figures.

As shown on the figures, the predicted surges were in rather good agreement with the data both with and without the surge tank. The worst agreement occurred when the inflow rates were below about 0.4 cfs (11,000 cc/sec) with the predicted surges generally being greater than the observed surges (except for the reaches which included a surge tank). It has previously been pointed out that data were not taken to determine the head loss for this low range of discharges and that the head loss was probably higher than that used for the predicted surges, (Equations 10a and 11a). An

increase in the head loss used in the analysis would increase the damping coefficient ( $R$ ) and thus reduce the magnitude of the predicted surges. It has also been pointed out that the surge tank was not very sensitive to the value of  $R$ . Thus, an increase in  $H_L$  and  $R$  would not significantly affect these latter predictions.

Comparison with unsteady inflow. --Data were available for the high head loss condition from some tests which had been made previously with an unsteady inflow where the discharge was increased in an essentially linear fashion from zero to 0.153 (4,330 cc/sec) by a specially designed valve. Figure 20 compares surges measured for various steady inflows with the surges which took place for the same inflow under unsteady conditions. The figure shows surge data for gate-opening time of 2,880 sec. and 195 sec. Although this is a rather limited comparison, it appears that for the longer opening time, the surges were approximately equal in magnitude to those obtained with steady inflows. Thus, the surges for the longer opening time were apparently not influenced by the unsteadiness of the inflow but rather were due to the same causes as the surges with steady inflow. On the other hand, the surges with the shorter opening time were larger for the unsteady flow. Thus, there was apparently some additional surging associated with the unsteady inflow.

Methods of surge control. --When all reaches of pipe between successive pipe checks are identical, the various reaches have the same natural period of oscillation, and  $T_r$  is equal to unity from one reach to the next. A pipe system of this type is essentially a surge amplifier and has nothing in it to cause surge reduction except frictional resistance. However, for economic reasons, a pipe is usually designed to keep friction at a minimum so that there is little damping to control the surge magnitude.

Almost any change to make a pipe reach have a natural frequency different from the preceding reach will cause  $T_r$  to be different from unity and thus help reduce the surges relative to what they would be for identical reaches. However, the most benefit can be obtained by making  $T_r$  less than unity rather than greater than unity (see Figure 4). As  $T_r$  increases, the best condition that can be obtained (for low values of  $R$ ) is to have the surges in a reach of pipe equal to, but never less than, the inflow surges. On the other hand, as  $T_r$  decreases from unity, the magnitude of the surges may be made arbitrarily small by letting  $T_r$  become arbitrarily small. In particular, if  $T_r$  is less than 0.707, the surges are always less than the inflow surges regardless of the value of  $R$ . If it is assumed that the surges in each pipe reach occur at the natural frequency of the reach, then  $T_r$  can be kept small in at least two different ways: (1) by

making the pipe reaches successively longer or (2) by using surge tanks that are successively larger if the reaches are all the same lengths. This assumes that the flow in each reach oscillates at the natural frequency of that reach. This is not necessarily the situation though. If the oscillations are generated at the natural frequency of one reach, the flow will have to pass through several reaches before the frequency of surging changes. Thus, the length of the pipe or the size of the surge tank would probably not have to be changed in each pipe reach. (Recall that  $T_r$  was defined as the ratio of the inflow period to the natural period of the pipe reach and not as the ratio of two natural frequencies of two successive pipe reaches.)

A possible area for further study might be the investigation of the conditions under which the period of oscillation will change when the natural period of the pipe reaches is different from the period of the inflow.

In a previous report (Reference 2) of work done by the Bureau of Reclamation, another method was presented and analyzed for controlling surge magnitude. This method was essentially a means of causing two or more pipe reaches to act as a unit by covering the pipe checks between the reaches. At the same time, relief valves were used to limit the magnitude of both positive and negative pressures which could develop under the covers. The system studied previously did not have air vents downstream of the pipe checks.

If enough head is available so that the damping coefficient  $R$  can be made greater than 0.6 (Figure 4), then surges will not be amplified regardless of the value of  $T_r$ . For discharges less than the design value, some of the available head is dissipated by water falling into the downstream legs of the pipe checks. This head loss is not effective in damping the surges. If part of this head could be dissipated through the action of a boundary force such as partially closed gates, then the damping would be increased. The amount of opening of the gates would have to be increased as the inflow increased in order to pass the higher flows without overflowing the check structures. Such a system of variable gates could undoubtedly reduce surging, but the cost of installation and operation of the gates would probably be prohibitive.

The discussion above has concerned possible means of preventing the magnitude of surging from becoming too large. Another approach to surge control might be to eliminate the disturbances which initiate the surges. As discussed earlier, it is felt that the surges in the present study were initiated by release of entrapped air. It

might be possible to find means of releasing the air so that no surging would be initiated due to this cause. However, there are many other possible disturbances that can start surges. It would probably never be possible to eliminate them all, especially since changes in delivery rates can cause surging. Thus, it seems more practical to focus attention on means of controlling surge magnitude rather than trying to eliminate all the possible causes of surging.

## REFERENCES

1. Olander, H. C., "Hydraulic Design Features of the Canadian River Aqueduct," paper presented before Texas Section, ASCE, Fort Worth, Texas, October 7-9, 1965. Published by Office of Chief Engineer, Bureau of Reclamation, Denver, Colorado
2. Hale, C. S. et al, "Surge Control on the Coachella Pipe Distribution System," Engineering Monograph 17, Bureau of Reclamation, Denver, Colorado, 33 pages, January 1954
3. Freberg, C. R. and E. N. Kemler, Elements of Mechanical Vibration, 2nd Edition, Wiley, 227 pages, 1957
4. McNowen, J. S., "Surges and Water Hammer," Chapter 7 in Engineering Hydraulics, edited by H. Rouse, Wiley, New York, 1950
5. Scarborough, J. B., Numerical Mathematical Analysis, 5th Edition, Johns Hopkins Press, Baltimore, 1962
6. Colgate, D., "Hydraulic Model Studies of the Flow Characteristics and Air Entrainment in the Check Towers of the Main Aqueduct, Canadian River Project, Texas," Report Hyd-555, Hydraulic Branch, Office of Chief Engineer, Bureau of Reclamation, Denver, Colorado, 12 pages and 15 figures, June 1, 1966
7. Moseley, D. S., "Measurement Error in the Orifice Meter on Pulsating Water Flow," Flow Measurement Symposium, ASME, 345 East 47th Street, New York, pages 103-123, 1966

## APPENDIX

### COMPUTER PROGRAM

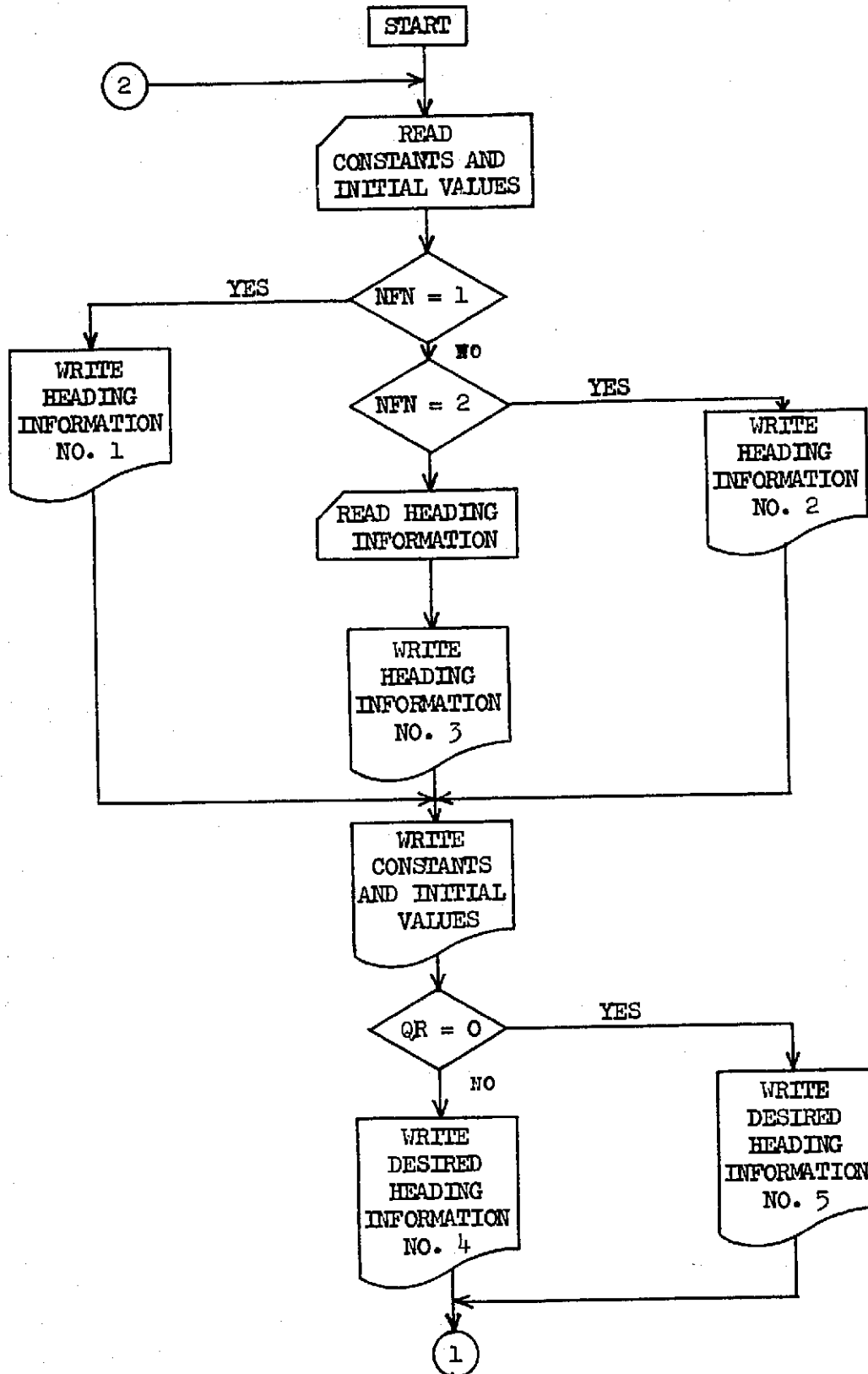
The following computer program was written to solve a nonlinear equation of the type:

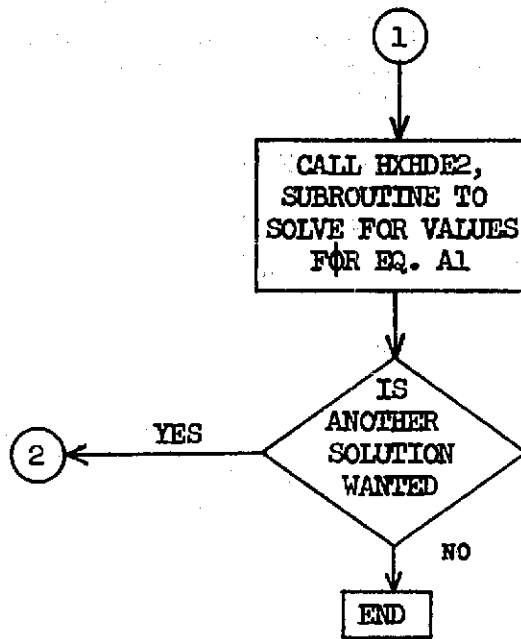
$$\frac{d^2 Q'}{dt'^2} = -4\pi R T_r |Q'| \frac{dQ'}{dt'} - 4\pi^2 T_r^2 Q' + 4\pi^2 T_r^2 Q_{in} \quad A1$$

A Runge-Kutta technique as presented by J. B. Scarborough on page 358 of "Numerical Mathematical Analysis," 5th Edition, is used for the solution.

Program variables are defined in the program which follows the flow chart.

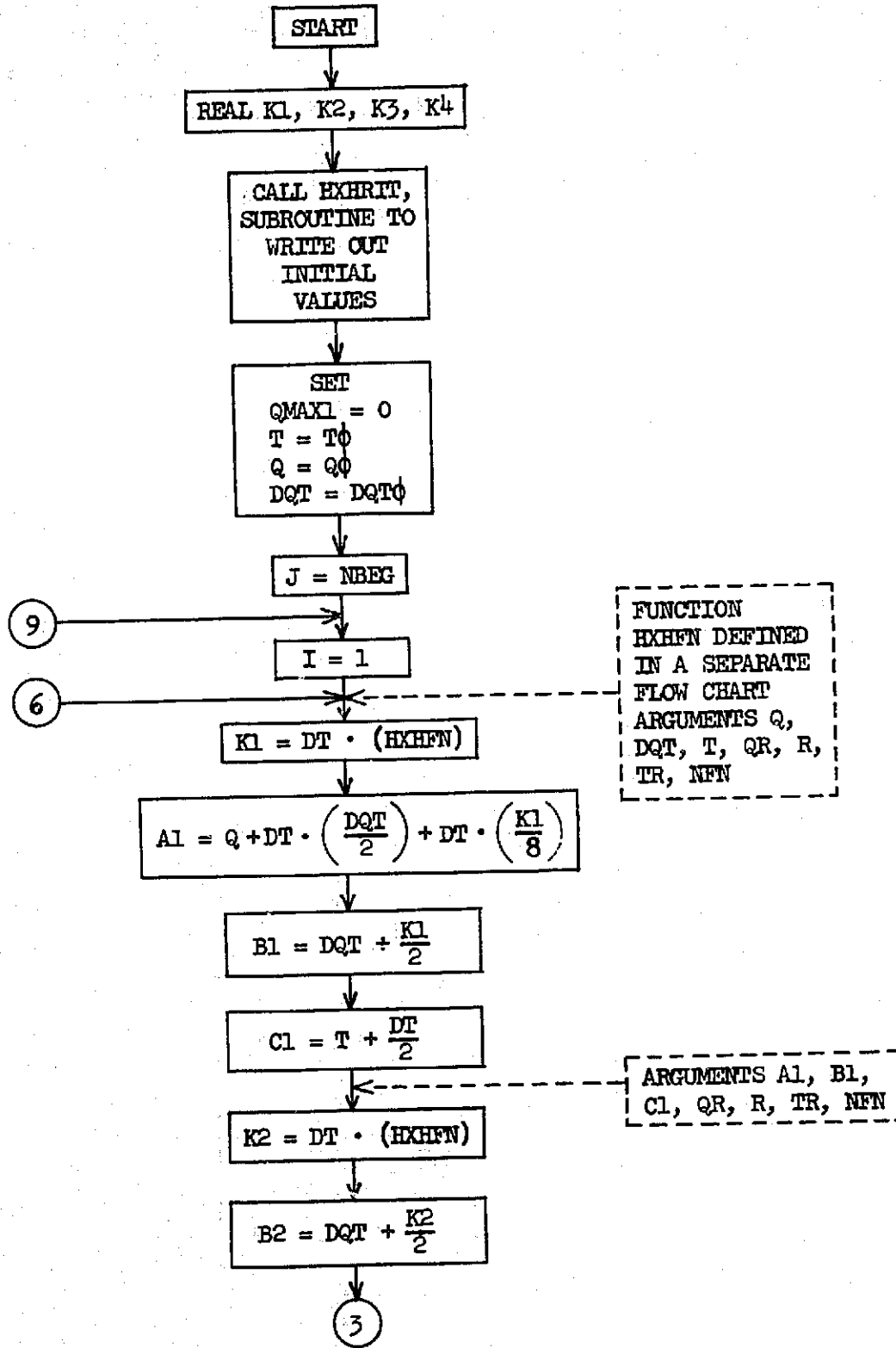
PROGRAM HXHSRG

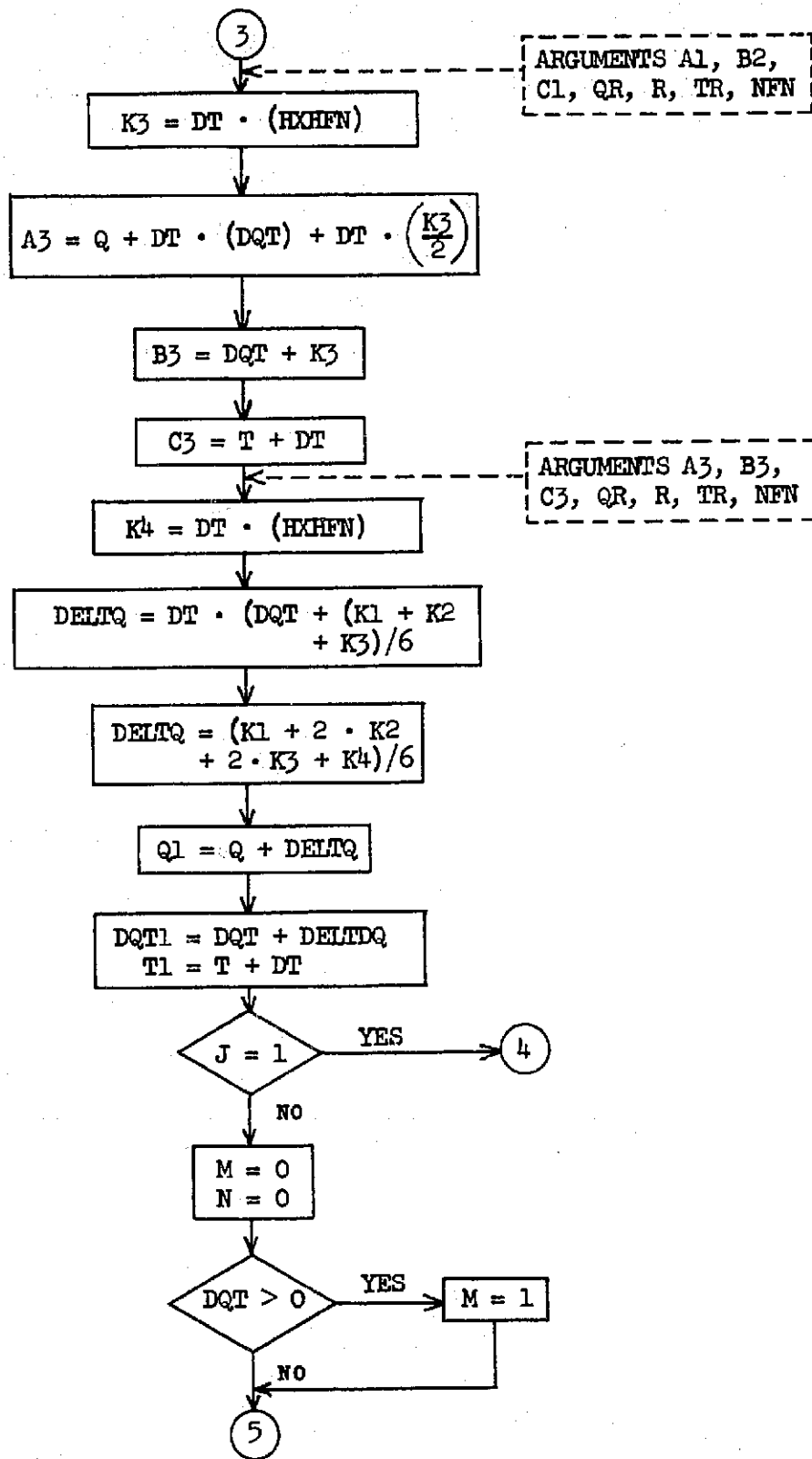


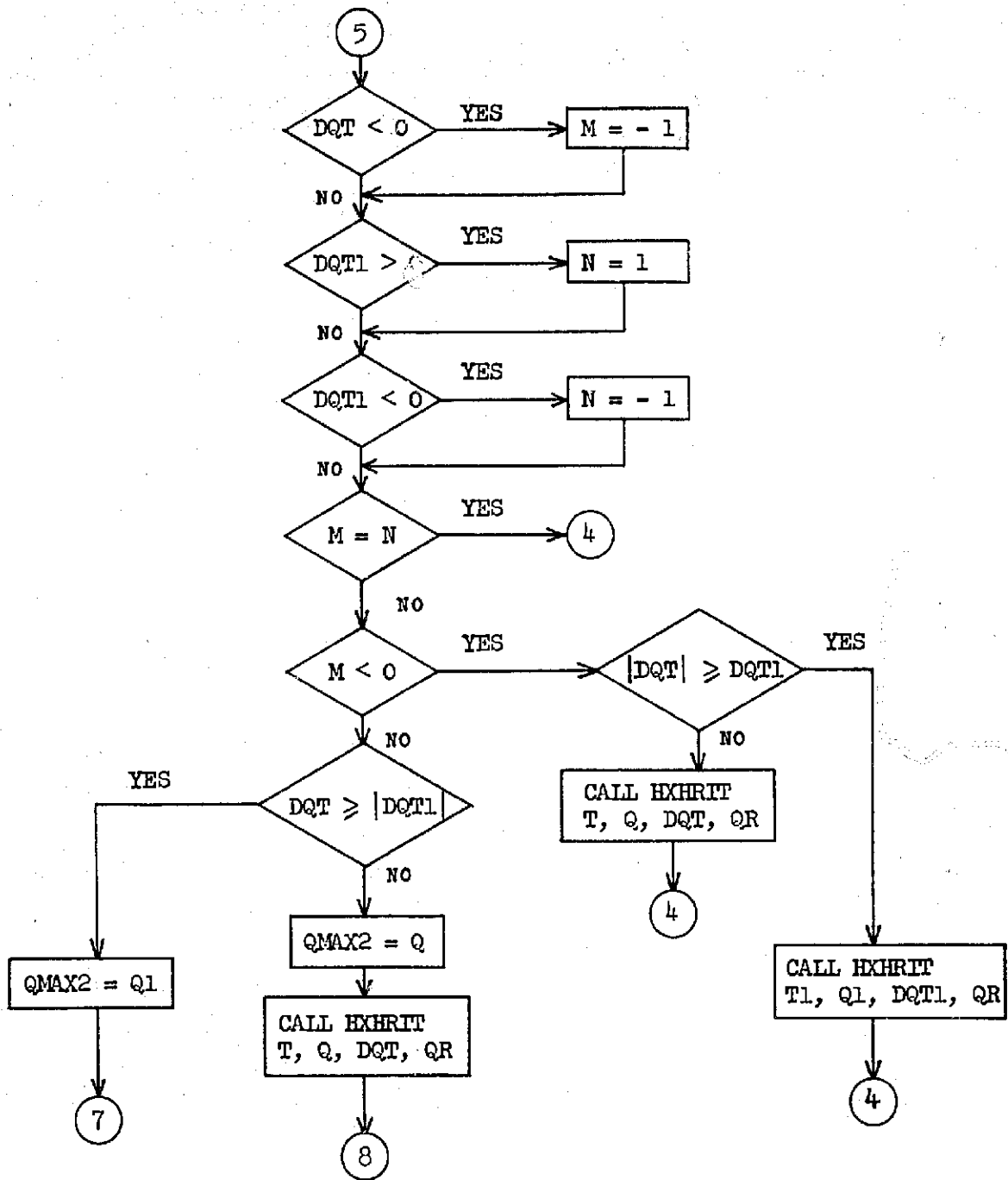


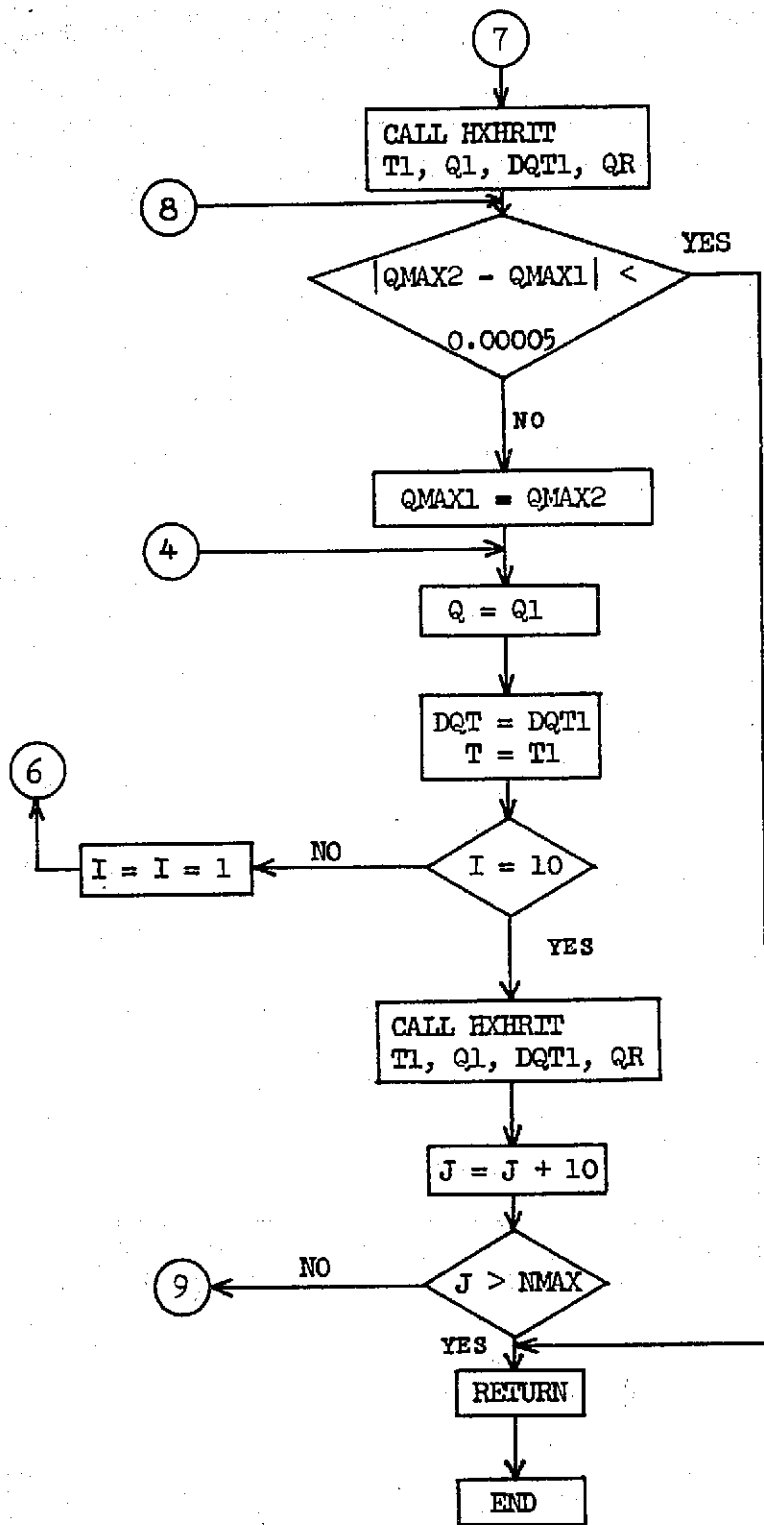
SUBROUTINE HXHDE2

ARGUMENTS Q0, DQTO, TO, DT, NBEG,  
NMAX, QR, R, TR, NFN

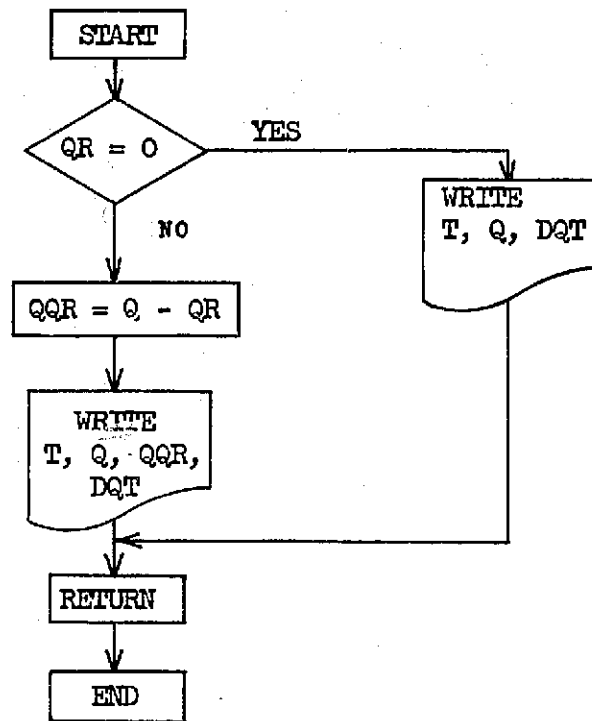






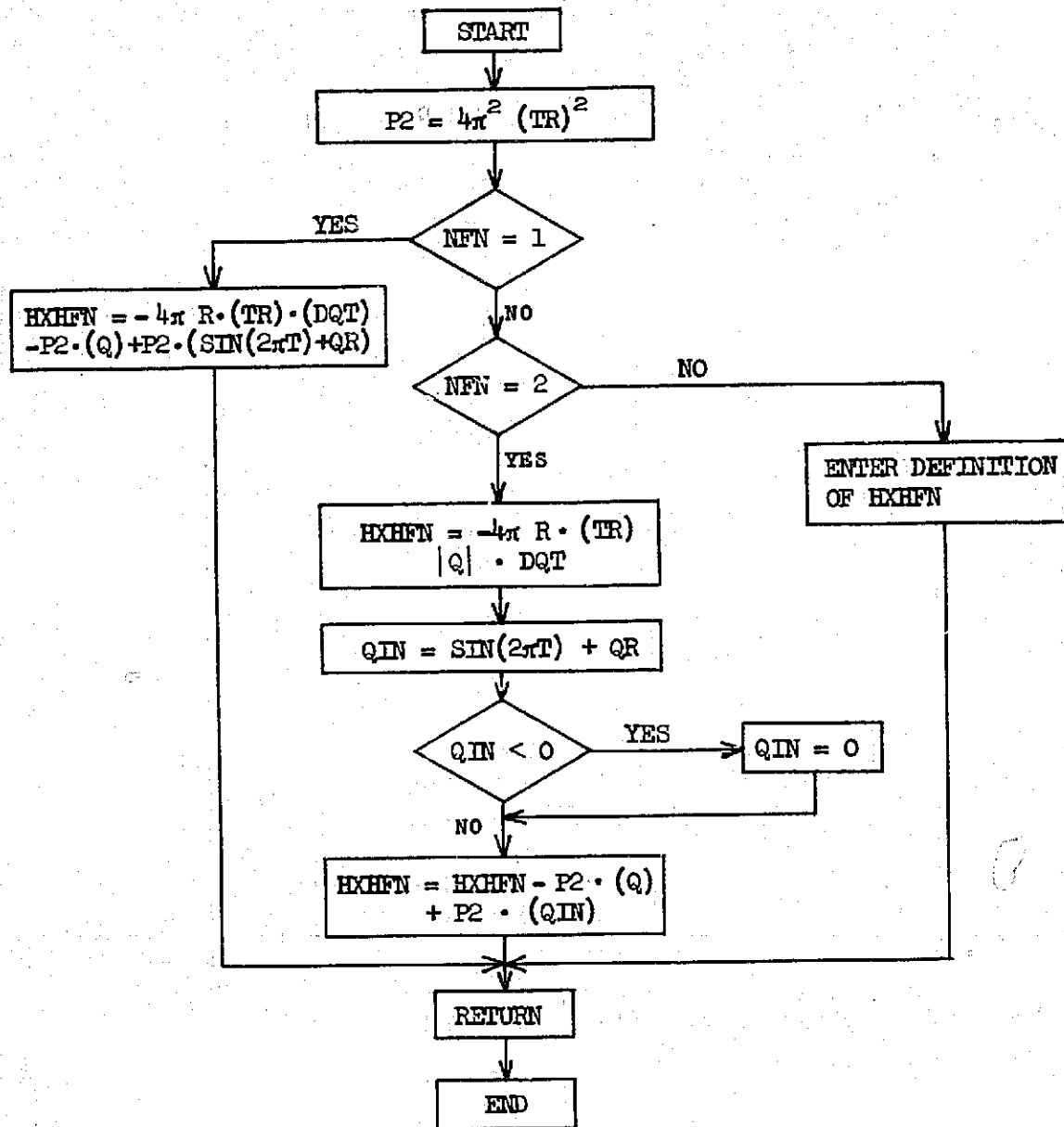


SUBROUTINE HXRIT  
ARGUMENTS T, Q, DQT, QR



FUNCTION HXHFN

ARGUMENTS Q, DQT, T, QR, R, TR, NFN



```

PROGRAM HXHSRG
C NUMERICAL INTEGRATION OF NON-LINEAR MOMENTUM EQUATION (EQ 6, HYD580)
C
C FORTRAN
C
C READ CONSTANTS AND INITIAL VALUES IN STATEMENT 5.
C SEE DEFINITIONS IN STATEMENT 20.
C TO, QO, DQTO = INITIAL VALUES OF T, Q, DQT, WHERE DQT = DQ/DT
C NFN=1 GIVES LINEAR DAMPING, NFN=2 GIVES SQUARE-LAW DAMPING, NFN=3
C GIVES DAMPING AND INFLOW AS SPECIFIED IN FUNCTION
C SUBPROGRAM HXHFN FOLLOWING STATEMENT 30.
C IF NFN = 3, 2 CARDS MUST BE READ IN STATEMENT 15 OF MAIN PROGRAM,
C THE INFORMATION ON THESE CARDS WILL BE LISTED AS PART OF THE OUTPUT
C AND MAY BE USED TO DESCRIBE THE DAMPING AND INFLOW USED IN THE
C FUNCTION SUBPROGRAM HXHFN FOLLOWING STATEMENT 30.
C INTEGRATION STOPS WHEN PERIODIC FLOW IS OBTAINED IN PIPE OR WHEN
C T = DT*NMAX, WHICHEVER COMES FIRST.
C (NMAX - NBEG)*DT = MAX. NO. OF PERIODS OVER WHICH INTEGRATION WILL BE
C DONE. NORMALLY, NBEG = 1.
C
      DIMENSION SPEC(20)
      5 READ (2,10) QR, R, TR, DT, NBEG, NMAX, TO, QO, DQTO, NFN
      10 FORMAT (4F9.5, 2I6, 3F9.6, I3)
         IF (EOF,2) 9999,101
101 CONTINUE
      GO TO (11,13,15) NFN
      11 WRITE (3,12)
      12 FORMAT (1H1, 4X, 72H LINEAR DAMPING WITH FORCING FUNCTION PROPORTI
         ONAL TO SIN(2.*PI*T) + QR )
         GO TO 18
      13 WRITE (3,14)
      14 FORMAT (1H1, 4X, 76H SQUARE-LAW DAMPING WITH FORCING FUNCTION PROP
         ORTIONAL TO SIN(2.*PI*T) + QR )
         GO TO 18
      15 READ (2,16) (SPEC(I), I=1,20)
      16 FORMAT (10A8 / 10A8)
         WRITE (3,17) (SPEC(I), I=1,20)
      17 FORMAT (1H1, 4X, 10A8 / 5X, 10A8)
      18 CONTINUE
         WRITE (3,20) QR, R, TR, DT, TO, QO, DQTO
      20 FORMAT ( /
      1 5X, 61H QR = AVG. INFLOW/AMPLITUDE OF OSCILLATING INFLOW COMPONEN
      2T = , F9.5 //
      3 5X, 22H R = DAMPING FACTOR = , F9.5 //
      4 5X, 48H TR = INFLOW PERIOD/NATURAL PERIOD OF THE PIPE = , F9.5//
      5 5X, 47H DT = TIME INCREMENT IN NUMERICAL INTEGRATION = , F9.5//
      6 5X, 28H T = TIME/INFLOW PERIOD. /
      7 5X, 61H Q = DISCHARGE/AMPLITUDE OF OSCILLATING INFLOW COMPONE
      8NT. /
      9 5X, 57H DQ/DT = NONDIMENSIONAL ACCELERATION IN TERMS OF Q AND T.
      A // 5X, 22H INITIAL VALUES - T = , F9.5, 6H, Q = , F9.5,
      B 10H, DQ/DT = , F9.5 //)
         IF (QR .EQ. 0.0) GO TO 40
         WRITE (3,30)

```

30 FORMAT (9X, 2H T , 10X, 2H Q , 8X, 5H Q-QR , 7X, 6H DQ/DT)

GO TO 60

40 WRITE (3,50)

50 FORMAT (9X, 2H T , 10X, 2H Q , 8X, 6H DQ/DT / )

60 CONTINUE

CALL HXHDE2(QO, DQTU, TO, DT, NBEG, NMAX, QR, R, TR, NFN)

GO TO 5

9999 CONTINUE

CALL EXIT

END

```

SUBROUTINE HXHDE2(Q0, DQTO, TO, DT, NBEG, NMAX, QR, R, TR, NFN)
REAL K1, K2, K3, K4
CALL HXHRIT (TO, Q0, DQTO, QR)
QMAX1 = 0.0
T = TO
Q = Q0
DQT = DQTO
DO 1000 J = NBEG, NMAX, 10
DO 900 I = 1, 10
K1 = DT*HXHFN(Q, DQT, T, QR, R, TR, NFN)
A1 = Q + DT*DQT/2. + DT*K1/8.
B1 = DQT + K1/2.
C1 = T + DT/2.
K2 = DT*HXHFN(A1, B1, C1, QR, R, TR, NFN)
B2 = DQT + K2/2.
K3 = DT*HXHFN(A1, B2, C1, QR, R, TR, NFN)
A3 = Q + DT*DQT + DT*K3/2.
B3 = DQT + K3
C3 = T + DT
K4 = DT*HXHFN(A3, B3, C3, QR, R, TR, NFN)
DELTAQ = DT*(DQT + (K1 + K2 + K3)/6.)
DELTDQ = (K1 + 2.*K2 + 2.*K3 + K4)/6.
Q1 = Q + DELTAQ
DQT1 = DQT + DELTDQ
T1 = T + DT
IF (J .EQ. 1) GO TO 575
M = 0
N = 0
IF (DQT .GT. 0.) M = +1
IF (DQT .LT. 0.) M = -1
IF (DQT1 .GT. 0.) N = +1
IF (DQT1 .LT. 0.) N = -1
IF (M .EQ. N) GO TO 875
IF (M .LT. 0) GO TO 800
IF (DQT .GE. ABS(DQT1)) GO TO 750
QMAX2 = Q
CALL HXHRIT( T, Q, DQT, QR)
GO TO 760
750 QMAX2 = Q1
CALL HXHRIT( T1, Q1, DQT1, QR)
760 CONTINUE
IF (ABS(QMAX2 - QMAX1) .LT. 0.00005) GO TO 1100
QMAX1 = QMAX2
GO TO 875
800 IF (ABS(DQT) .GE. DQT1) GO TO 850
CALL HXHRIT( T, Q, DQT, QR)
GO TO 875
850 CALL HXHRIT( T1, Q1, DQT1, QR)
875 Q = Q1
DQT = DQT1
T = T1
900 CONTINUE
CALL HXHRIT( T1, Q1, DQT1, QR)

```

PAGE NO. 2

1000 CONTINUE  
301 FORMAT (1X, 3(4X, F8.3))  
1100 CONTINUE  
RETURN  
END

```
SUBROUTINE HXRIT( T, Q, DQT, QR)
IF (QR .EQ. 0.0) GO TO 100
QQR = Q - QR
WRITE (3,50) T, Q,QQR, DQT
50 FORMAT (1X, 4(4X,F8.3))
GO TO 300
100 WRITE (3,200) T, Q, DQT
200 FORMAT (1X, 3(4X,F8.3))
300 CONTINUE
RETURN
END
```

```
FUNCTION HXHFN(Q, DQT, T, QR, R, TR, NFN)
PI = 3.141593
P2 = 4.*PI*PI*TR*TR
GO TO (10,20,30), NFN
10 HXHFN = -4.*PI*R*TR*DQT - P2*Q + P2*(SIN(2.*PI*T) + QR)
GO TO 100
20 HXHFN = -4. * PI * R * TR * ABS(Q) * DQT
QIN = SIN(2.*PI*T) + QR
IF (QIN .LT. 0,0) QIN = 0,0
HXHFN = HXHFN - P2*Q + P2*QIN
GO TO 100
30 CONTINUE
C FOR NFN = 3, ANY DEFINITION OF HXHFN MAY BE PLACED HERE.
100 CONTINUE
RETURN
END
```

INPUT DATA

C THE FOLLOWING CARDS ARE TYPICAL INPUT DATA TO BE READ IN STATEMENT  
C 5 OF THE MAIN PROGRAM.

1.0	0.0568	1.0	0.01	1	2001	0.0	0.0	0.0	2
0.77	0.1288	1.0	0.01	1	2001	0.0	0.0	0.0	2

TYPICAL OUTPUT

SQUARE-LAW DAMPING WITH FORCING FUNCTION PROPORTIONAL TO  $\sin(2 \cdot \pi \cdot T) + QR$

$QR = \text{AVG. INFLOW/AMPLITUDE OF OSCILLATING INFLOW COMPONENT} = 2.00000$

$R = \text{DAMPING FACTOR} = .20000$

$TR = \text{INFLOW PERIOD/NATURAL PERIOD OF THE PIPE} = 1.10000$

$DT = \text{TIME INCREMENT IN NUMERICAL INTEGRATION} = .01000$

$T = \text{TIME/INFLOW PERIOD.}$

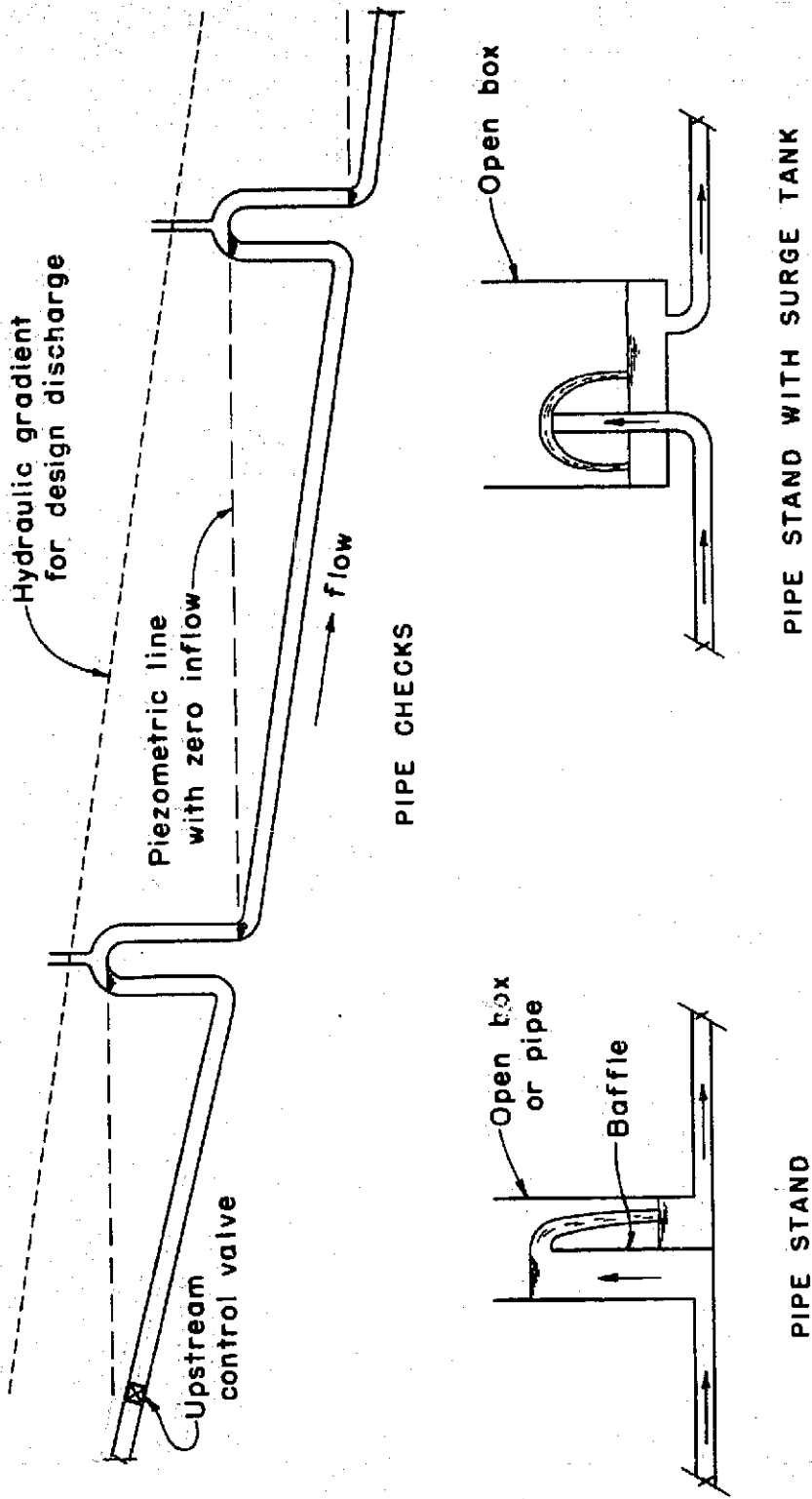
$Q = \text{DISCHARGE/AMPLITUDE OF OSCILLATING INFLOW COMPONENT.}$

$DQ/DT = \text{NONDIMENSIONAL ACCELERATION IN TERMS OF } Q \text{ AND } T.$

INITIAL VALUES -  $T = 0. \quad , \quad Q = 0. \quad , \quad DQ/DT = 0.$

T	Q	Q-QR	DQ/DT
0.	0.	-2.000	0.
.100	.500	-1.500	9.865
.200	1.775	-0.225	13.943
.300	2.966	0.966	8.856
.400	3.489	1.489	1.841
.430	3.518	1.518	0.128
.500	3.410	1.410	-3.063
.600	2.938	0.938	-6.110
.700	2.234	0.234	-7.740
.800	1.447	-0.553	-7.667
.900	0.784	-1.216	-5.097
.990	0.530	-1.470	-0.138
1.000	0.532	-1.468	0.546
1.100	0.941	-1.059	7.479
1.200	1.892	-0.108	10.461
1.300	2.819	0.819	7.294
1.400	3.282	1.282	1.962
1.440	3.321	1.321	0.025
1.500	3.245	1.245	-2.466
1.600	2.834	0.834	-5.548
1.700	2.179	0.179	-7.303
1.800	1.430	-0.570	-7.333
1.900	0.796	-1.204	-4.850
1.990	0.560	-1.440	-0.005
2.000	0.564	-1.436	0.662
2.100	0.975	-1.025	7.392
2.200	1.909	-0.091	10.250

T	Q	Q-QR	DQ/DT
2.300	2.817	0.817	7.154
2.400	3.272	1.272	1.932
2.440	3.310	1.310	0.022
2.500	3.235	1.235	-2.447
2.600	2.826	0.826	-5.519
2.700	2.174	0.174	-7.276
2.800	1.428	-0.572	-7.309
2.900	0.796	-1.204	-4.830
2.990	0.562	-1.438	0.009
3.000	0.565	-1.435	0.675
3.100	0.977	-1.023	7.391
3.200	1.911	-0.089	10.237
3.300	2.817	0.817	7.143
3.400	3.271	1.271	1.928
3.440	3.309	1.309	0.020
3.500	3.234	1.234	-2.446
3.600	2.826	0.826	-5.517
3.700	2.174	0.174	-7.274
3.800	1.428	-0.572	-7.308
3.900	0.796	-1.204	-4.828
3.990	0.562	-1.438	0.010
4.000	0.565	-1.435	0.676
4.100	0.977	-1.023	7.391
4.200	1.911	-0.089	10.236
4.300	2.818	-0.818	7.142
4.400	3.271	1.271	1.928
4.440	3.309	1.309	0.020



PIPE CHECKS

PIPE STAND WITH SURGE TANK

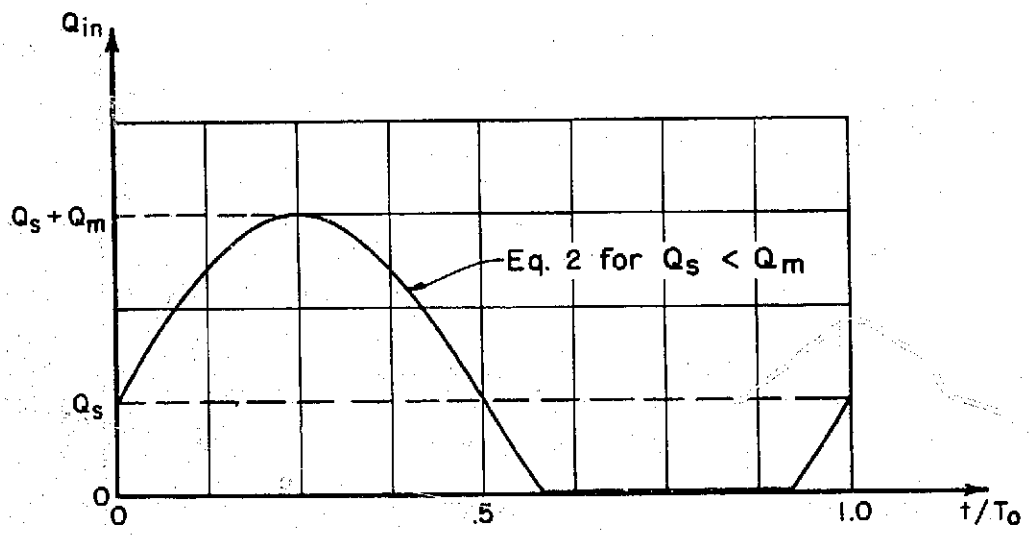
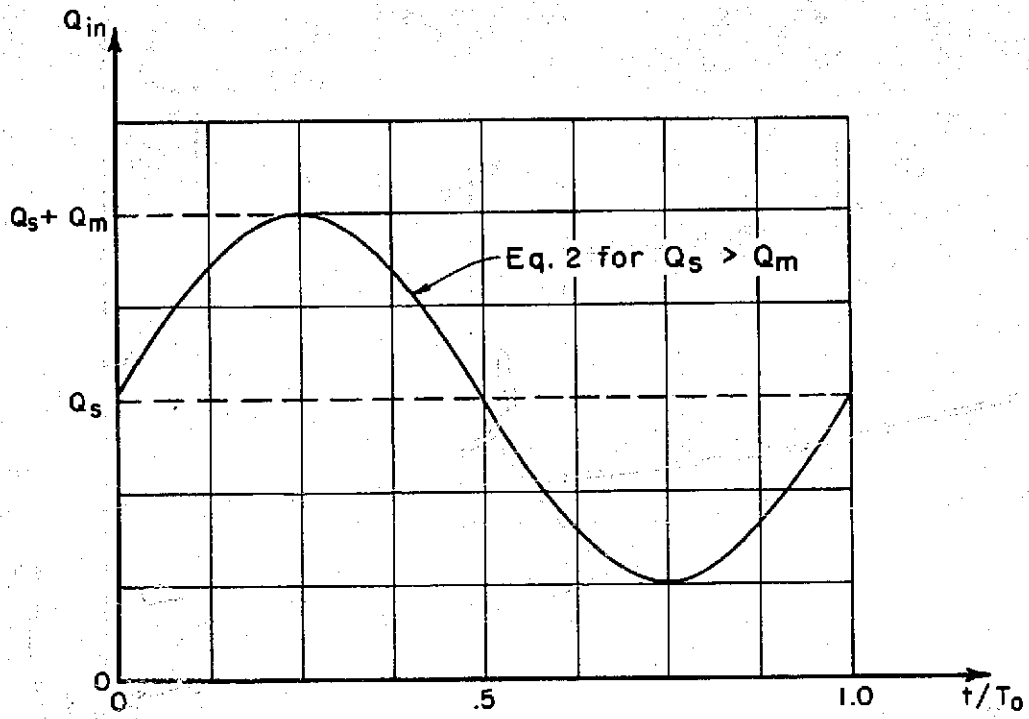
ELEVATIONS

PIPE LINE SURGES

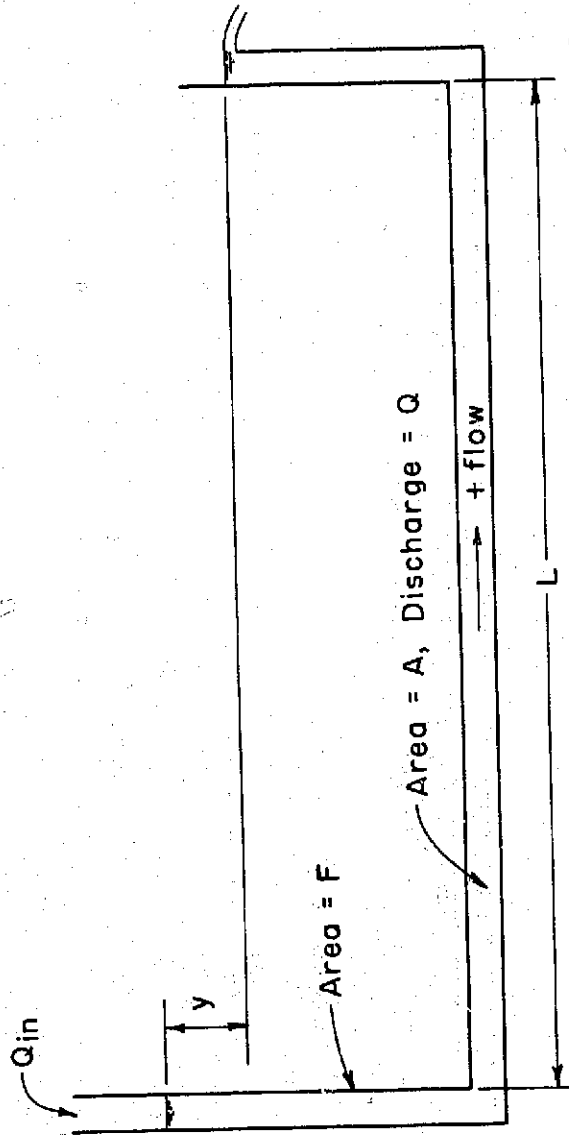
POSSIBLE TYPES OF CHECK STRUCTURES

PIPE STAND

FIGURE 2  
REPORT HYD-580

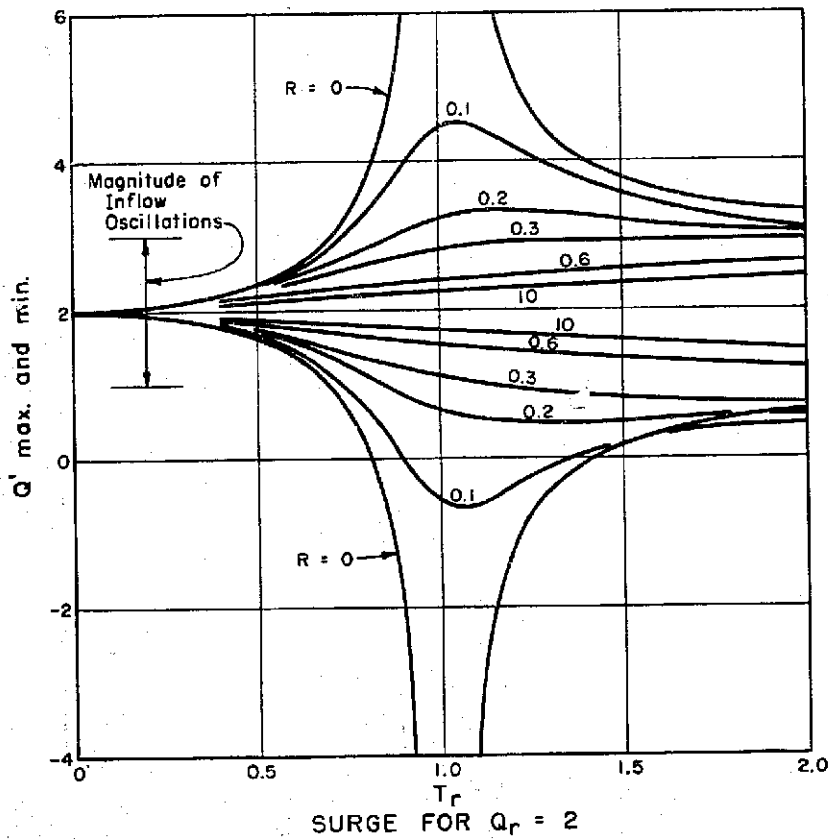
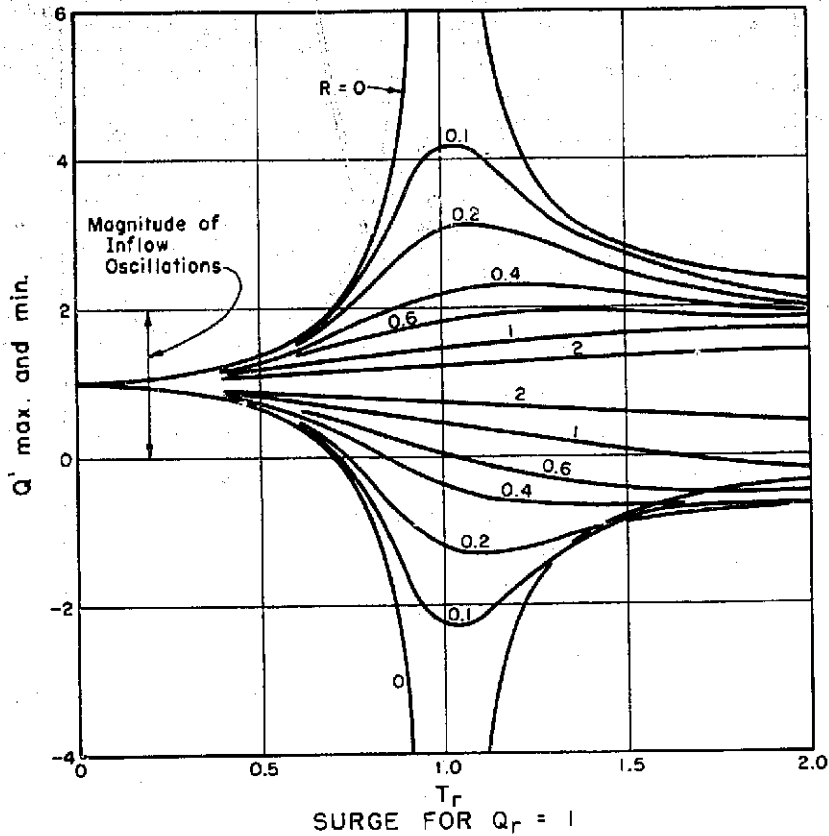


PIPE LINE SURGES  
PERIODIC INFLOW USED IN  
ANALYSIS OF SURGES

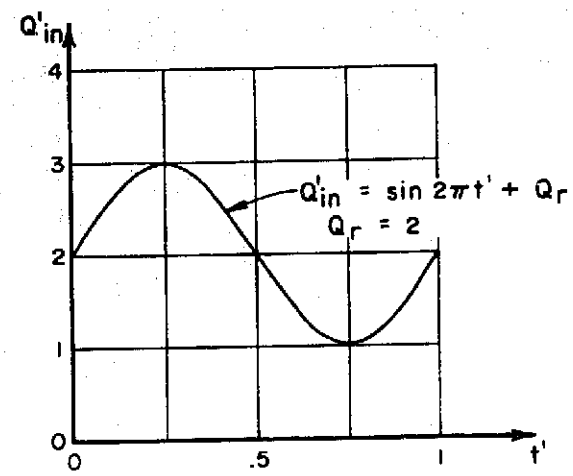


PIPE LINE SURGES  
DEFINITION SKETCH FOR DERIVATION  
OF DIFFERENTIAL EQUATION

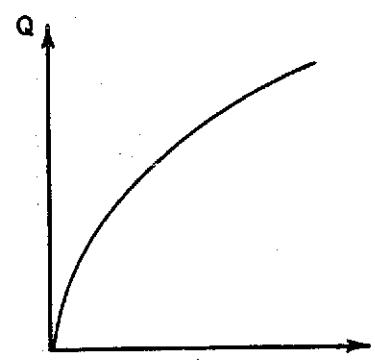
FIGURE 4  
REPORT HYD-580



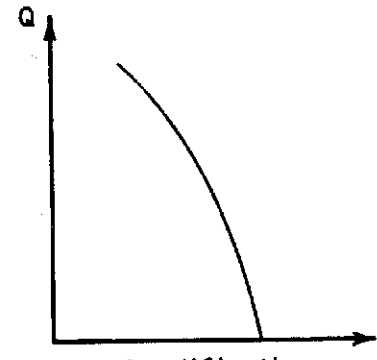
PIPE LINE SURGES  
MAGNITUDE OF DISCHARGE SURGES  
(CALCULATED FROM EQUATION 6)



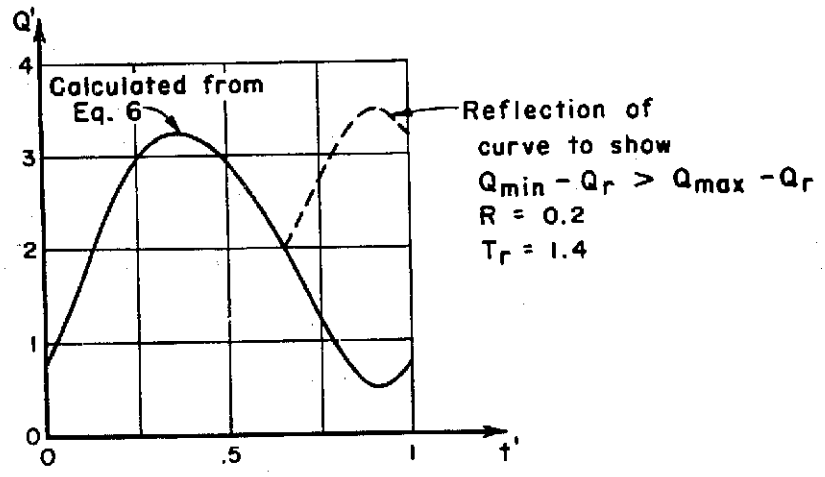
(a)



Damping  
(b)



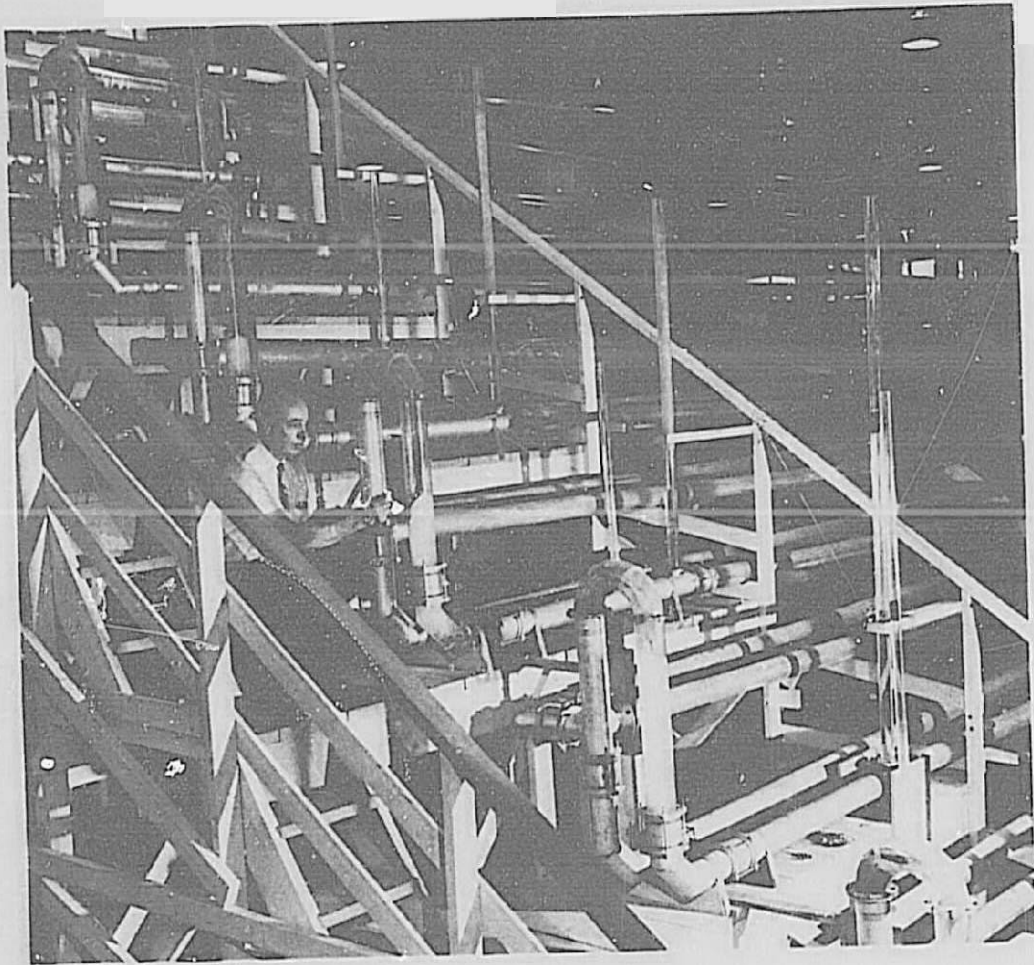
Amplification  
(c)



(d)

(a) plus (b) or (c) gives (d)

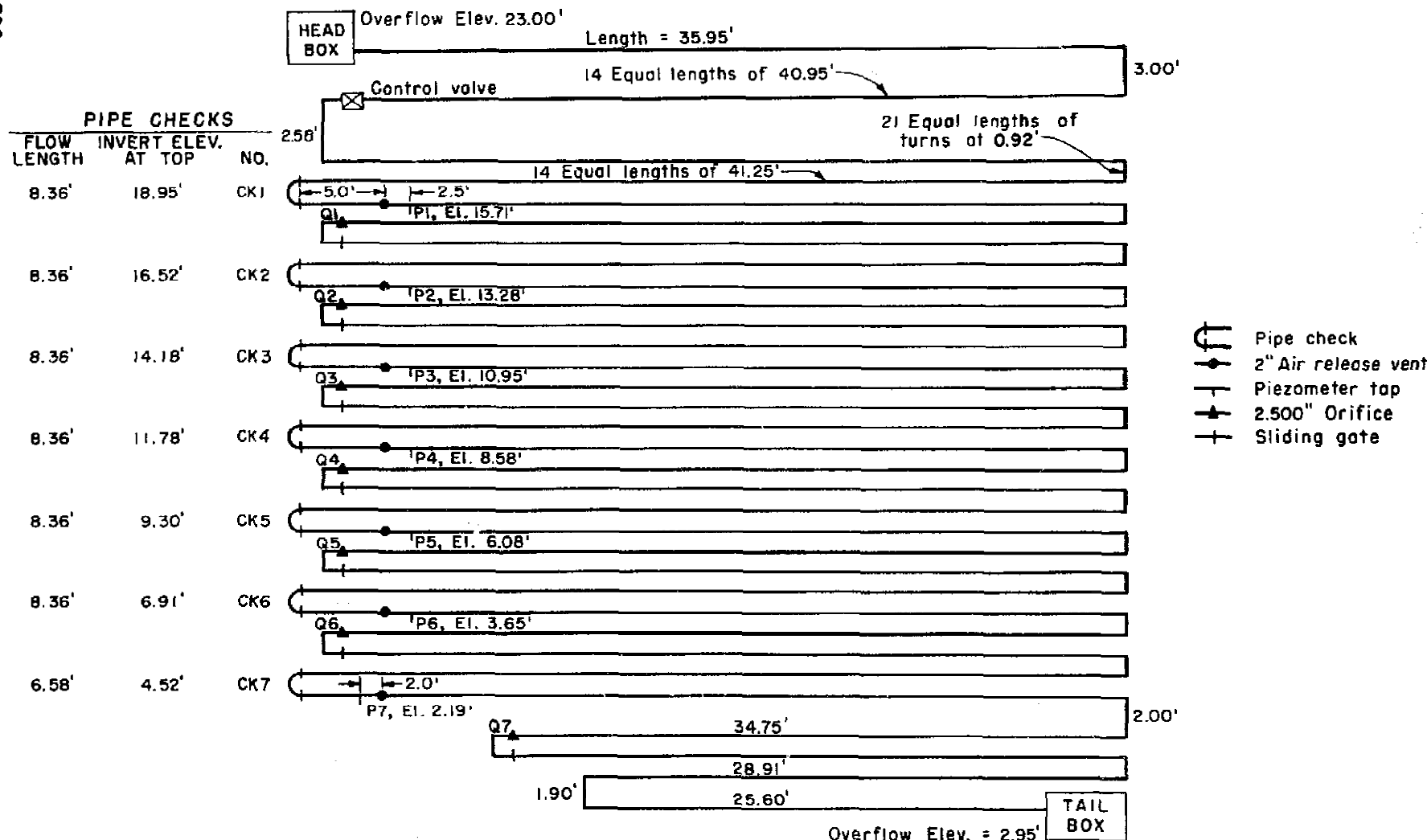
PIPE LINE SURGES  
ASYMMETRICAL SURGE RESULTING  
FROM VARIABLE DAMPING



Pipe Line Surges

EXPERIMENTAL PIPE SYSTEM

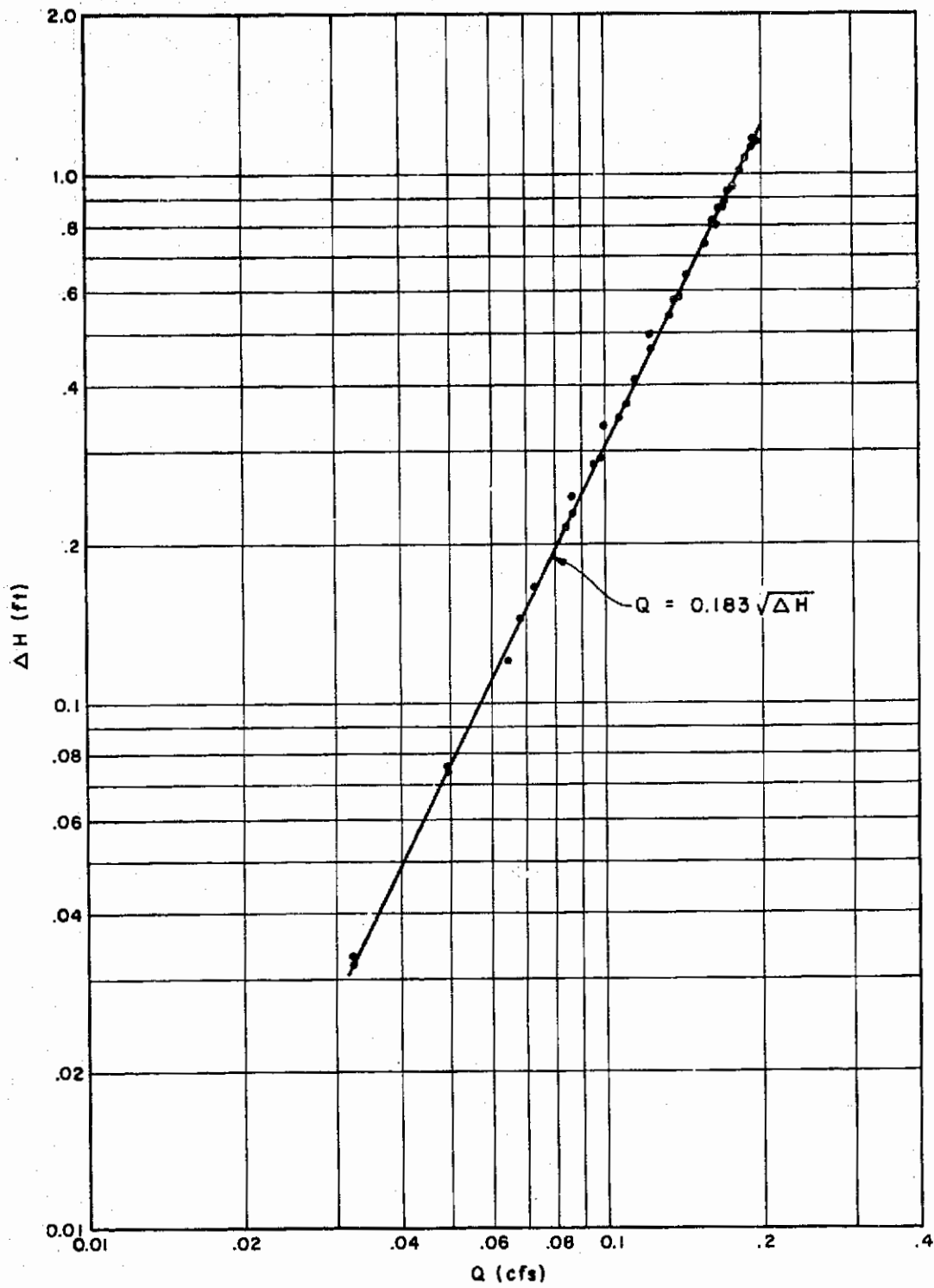
Photo PX-D-60622



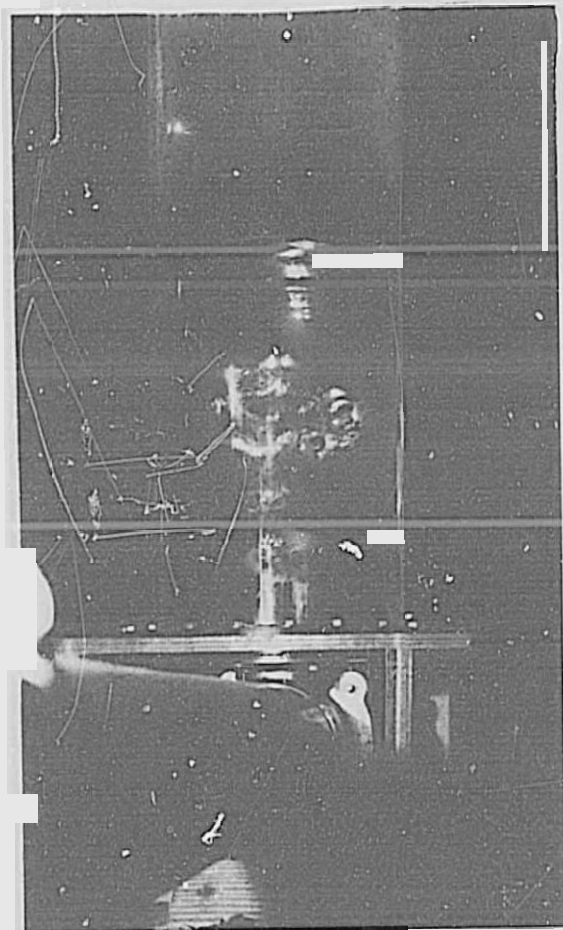
-  Pipe check
-  2" Air release vent
-  Piezometer tap
-  2.500" Orifice
-  Sliding gate

PIPE LINE SURGES  
SCHEMATIC DIAGRAM OF EXPERIMENTAL PIPE SYSTEM

FIGURE 8  
REPORT HYD-580



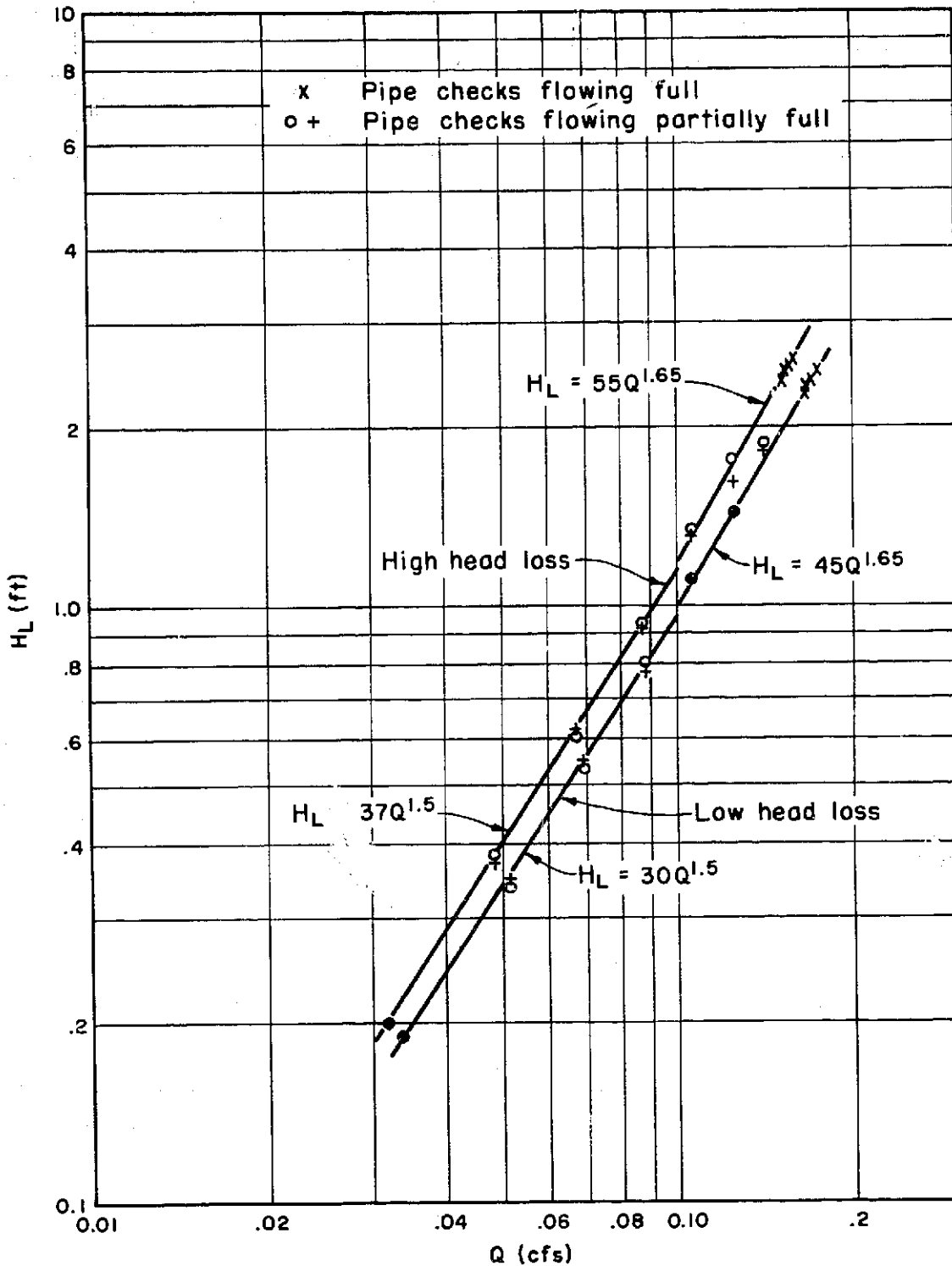
PIPE LINE SURGES  
CALIBRATION OF ORIFICE AT Q1



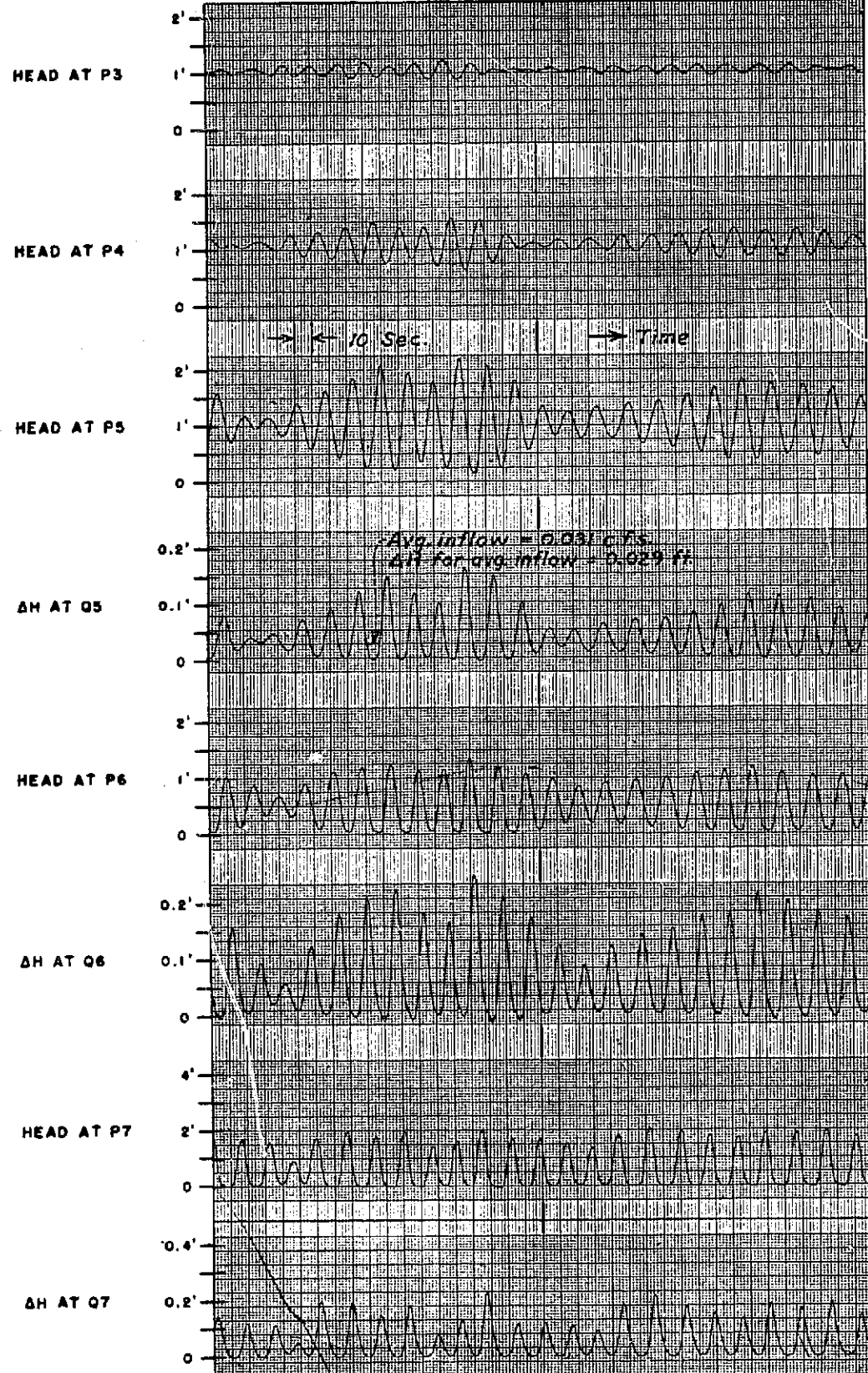
Pipe Line Surges  
SURGE TANK

Photo PX-D-60623

FIGURE 10  
REPORT HYD - 580



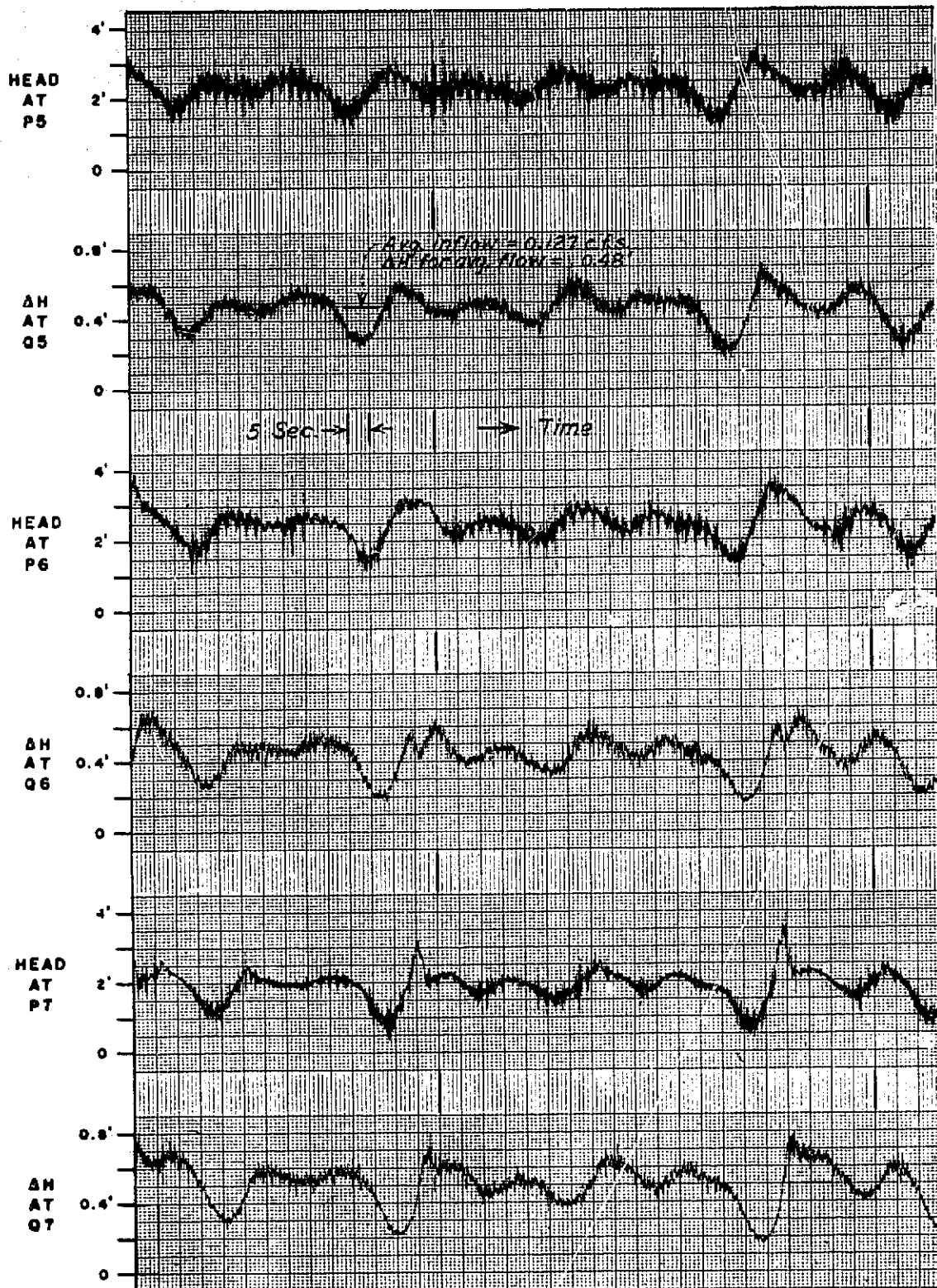
PIPE LINE SURGES  
HEAD LOSS VARIATIONS  
LOW AND HIGH HEAD LOSS CONDITIONS



Note - 1 second averaging used for these records

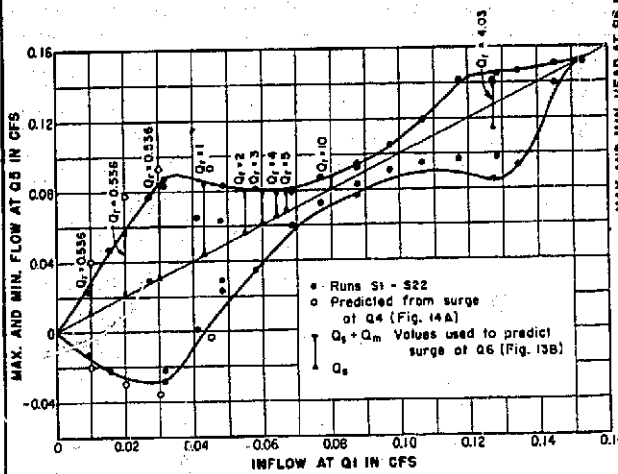
PIPE LINE SURGES  
OSCILLOGRAPH RECORD OF SURGES, RUN S69

FIGURE 12  
REPORT HYD-580

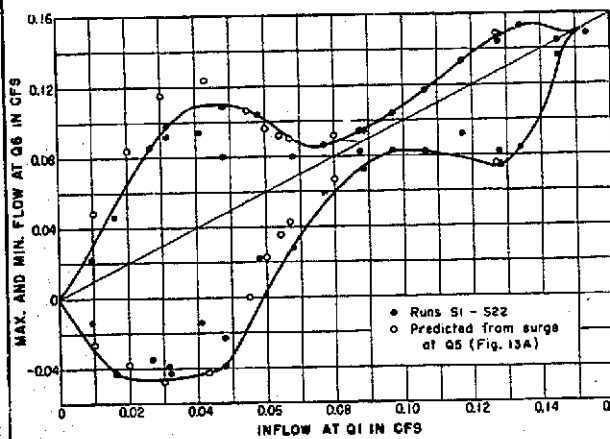


Note - 1 second averaging not used for these records

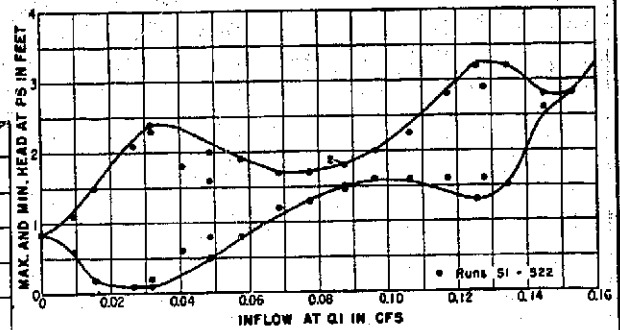
PIPE LINE SURGES  
OSCILLOGRAPH RECORD OF SURGES, RUN S19



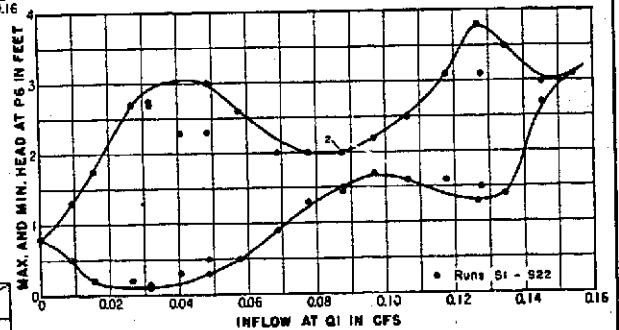
A. DISCHARGE SURGE AT Q5



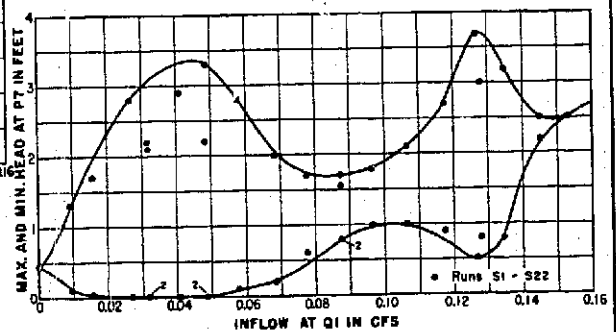
B. DISCHARGE SURGE AT Q6



C. HEAD SURGE AT P5



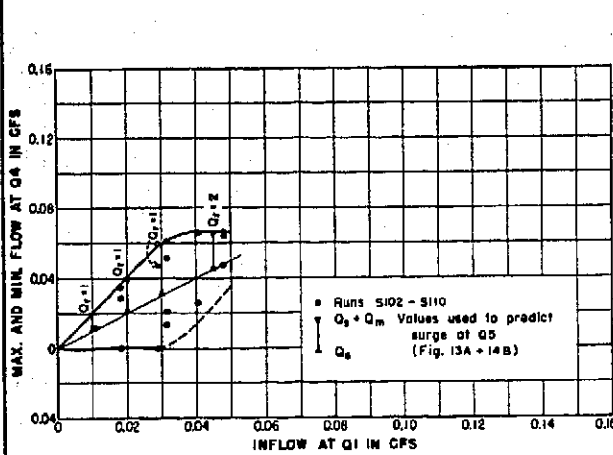
D. HEAD SURGE AT P6



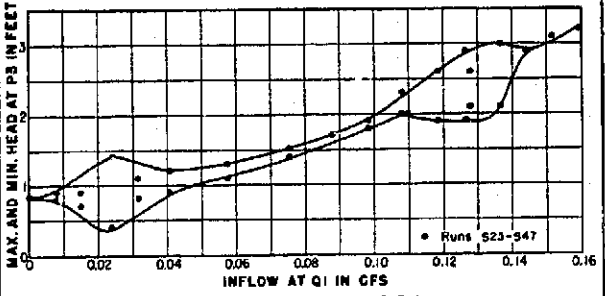
E. HEAD SURGE AT P7

PIPE LINE SURGES  
DISCHARGE AND HEAD SURGES  
WITH LOW HEAD LOSS AND WITHOUT SURGE TANK

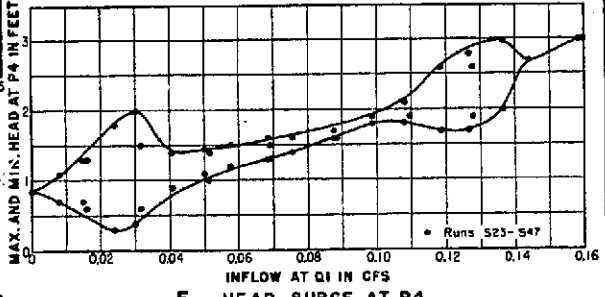
FIGURE 14  
REPORT HYD-580



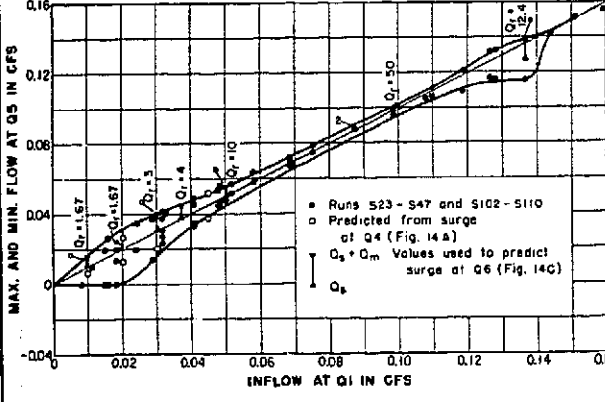
A. DISCHARGE SURGE AT Q4  
UPSTREAM OF SURGE TANK LOCATION



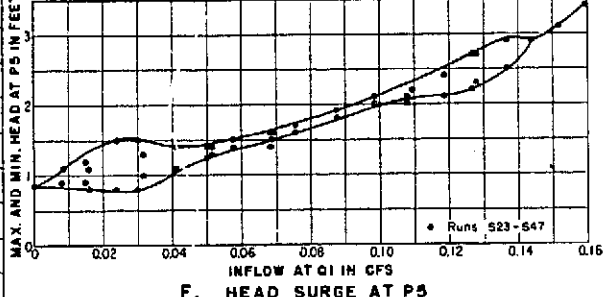
D. HEAD SURGE AT P3  
UPSTREAM OF SURGE TANK LOCATION



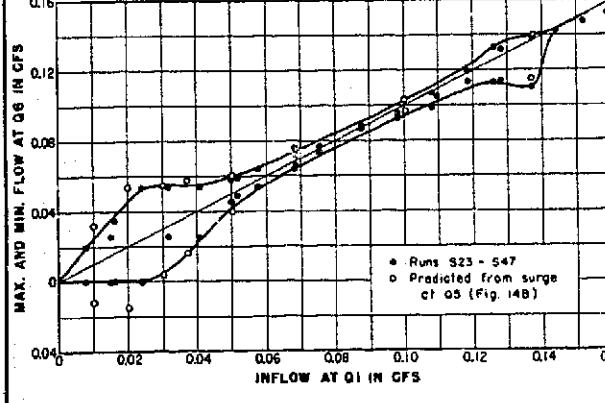
E. HEAD SURGE AT P4  
UPSTREAM OF SURGE TANK LOCATION



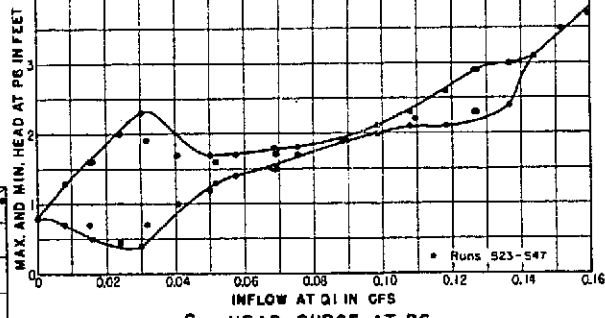
B. DISCHARGE SURGE AT Q5  
SURGE TANK IN REACH 5



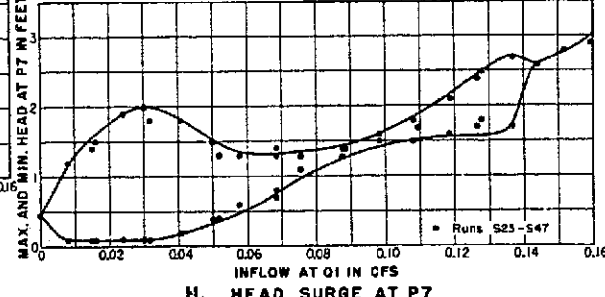
F. HEAD SURGE AT P5  
SURGE TANK IN REACH 5



C. DISCHARGE SURGE AT Q6  
SURGE TANK IN REACH 5

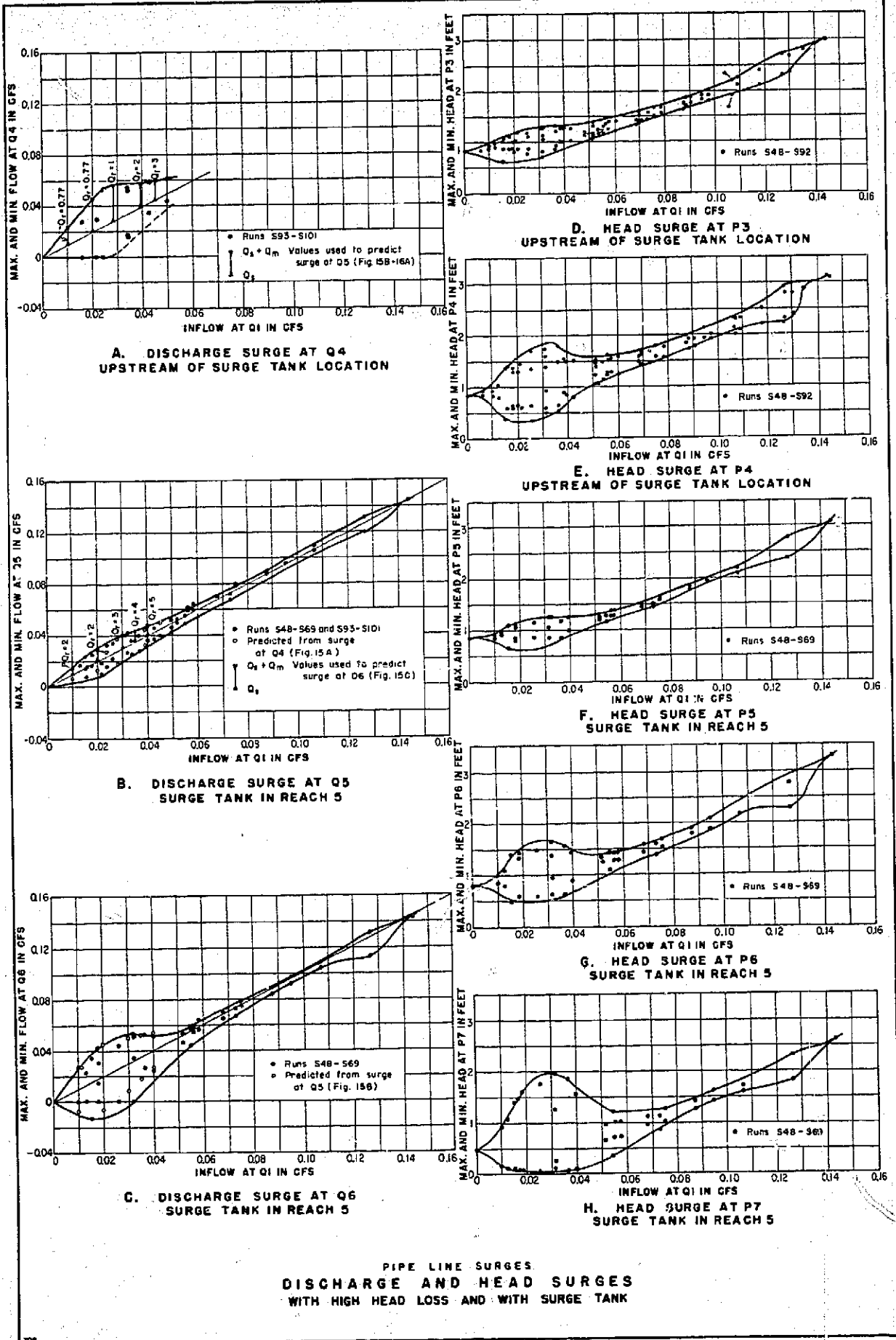


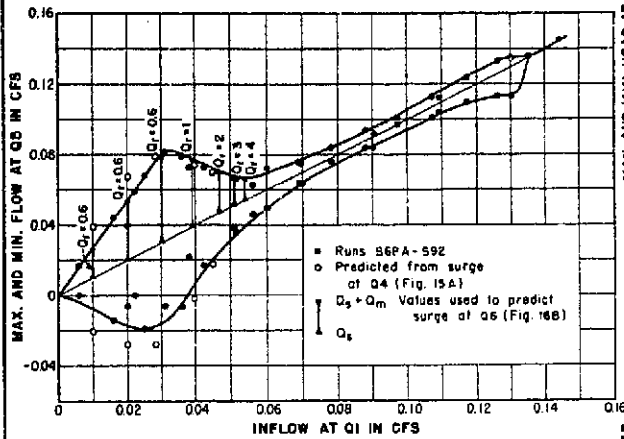
G. HEAD SURGE AT P6  
SURGE TANK IN REACH 5



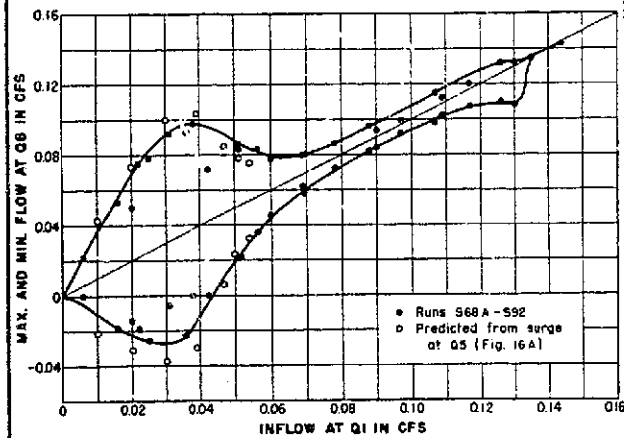
H. HEAD SURGE AT P7  
SURGE TANK IN REACH 5

PIPE LINE SURGES  
DISCHARGE AND HEAD SURGES  
WITH LOW HEAD LOSS AND WITH SURGE TANK

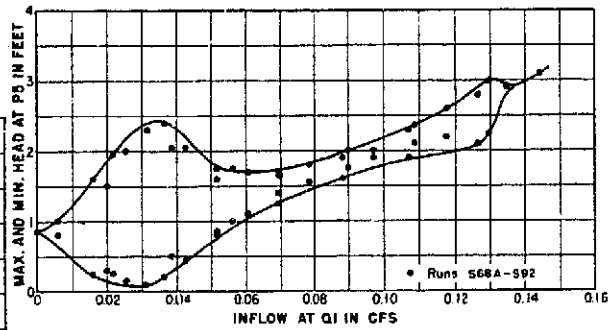




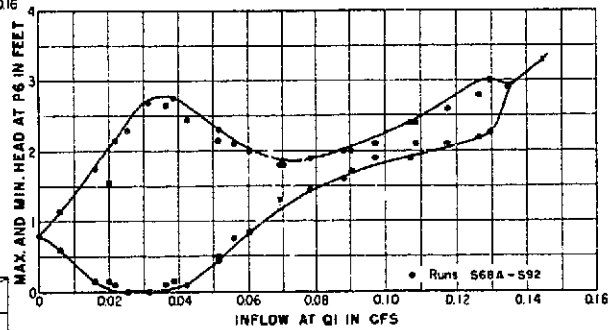
A. DISCHARGE SURGE AT Q5



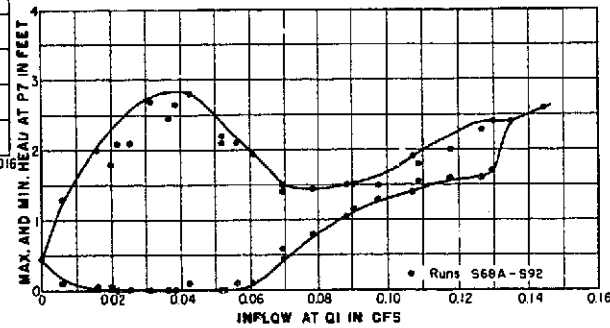
B. DISCHARGE SURGE AT Q6



C. HEAD SURGE AT P5

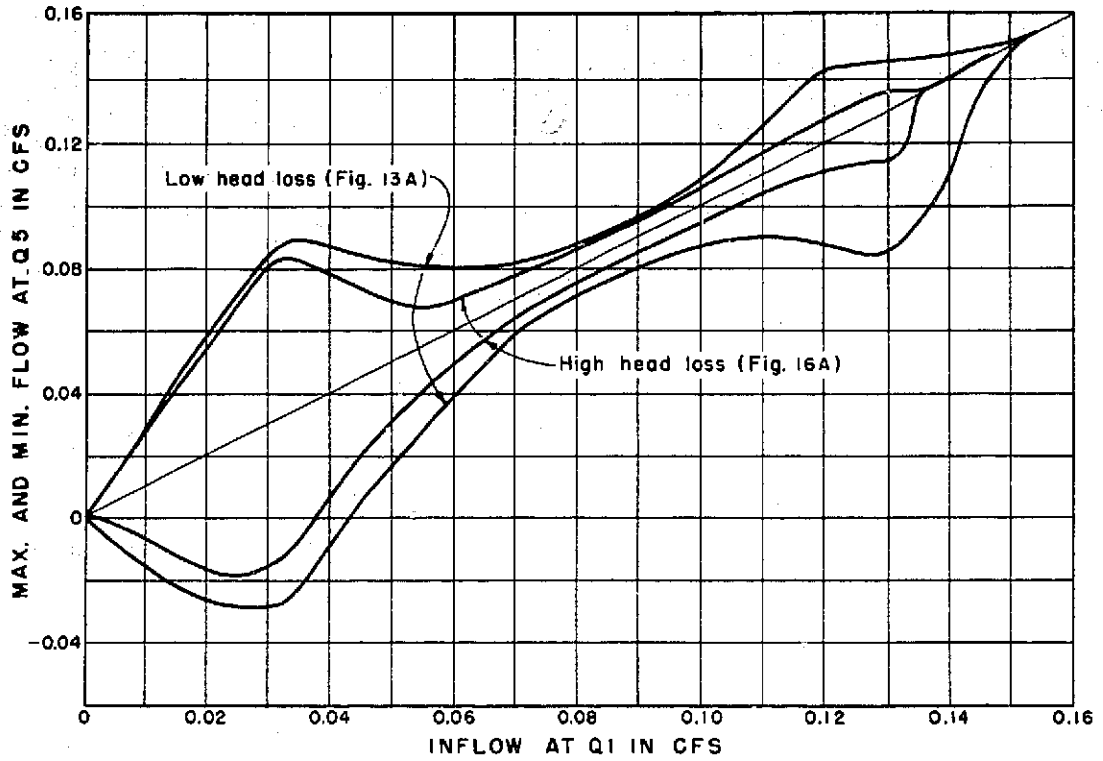


D. HEAD SURGE AT P6

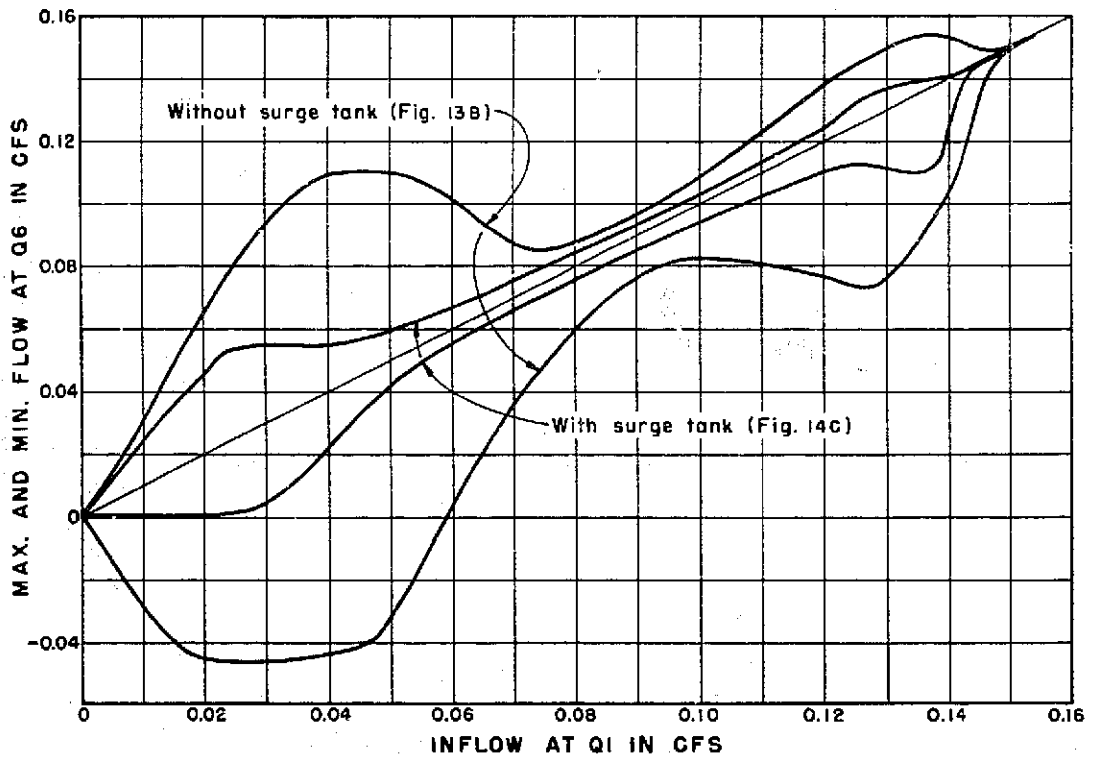


E. HEAD SURGE AT P7

PIPE LINE SURGES  
DISCHARGE AND HEAD SURGES  
WITH HIGH HEAD LOSS AND WITHOUT SURGE TANK



A. EFFECT OF HEAD LOSS ON SURGE AT Q5  
WITHOUT SURGE TANK

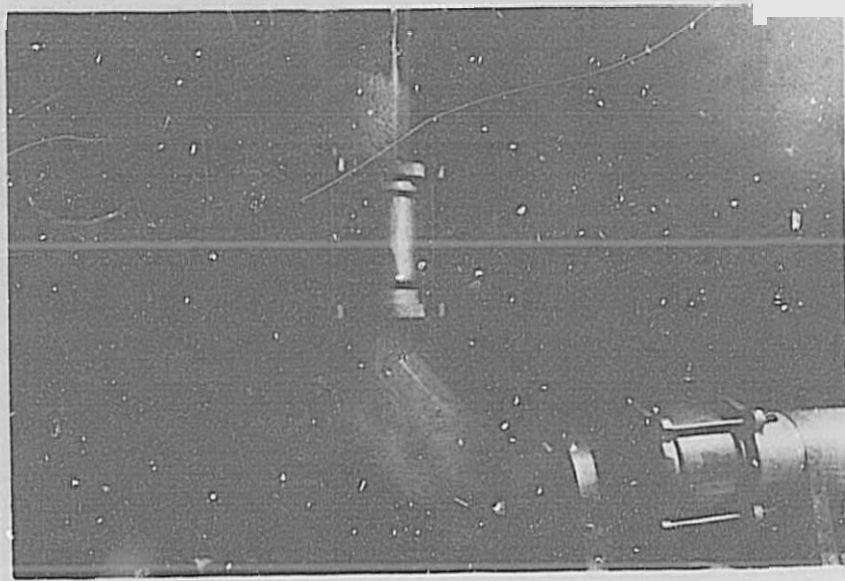


B. EFFECT OF SURGE TANK ON SURGE AT Q6  
WITH LOW HEAD LOSS

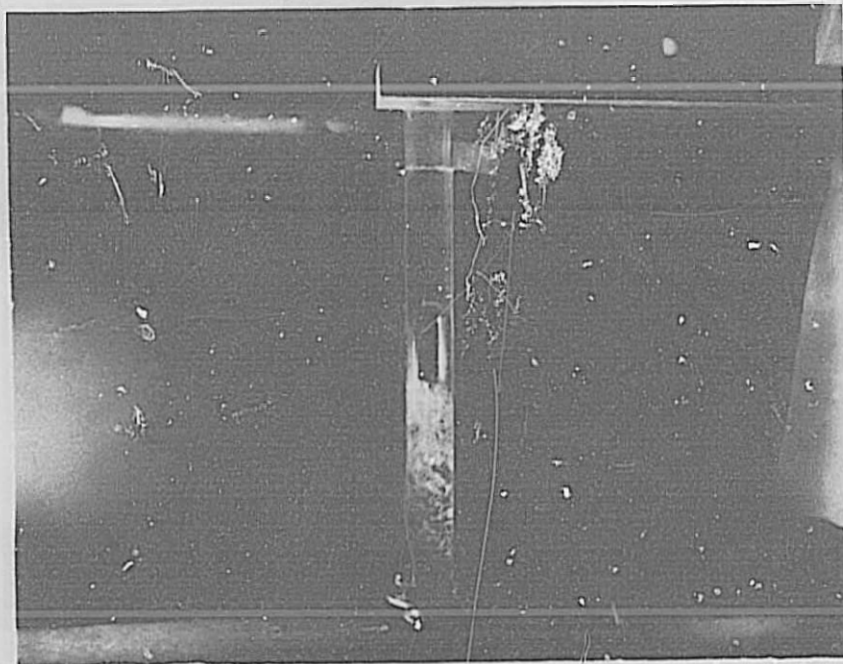
PIPE LINE SURGES

EFFECTS OF HEAD LOSS AND SURGE TANK ON SURGES

Figure 18  
Report Hyd-580



A. Air entrainment at downstream leg of pipe check.  
Photo PX-D-60624

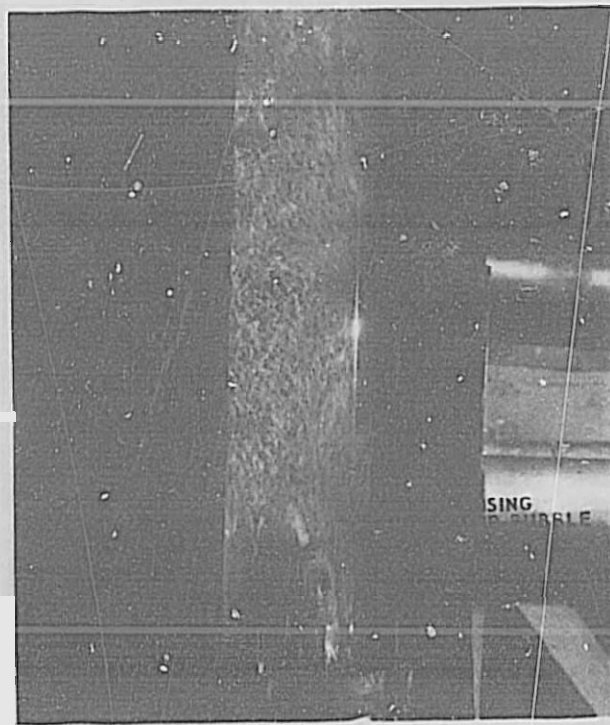


B. Release of air at 2-inch-diameter vent.  
Photo PX-D-60625

Pipe Line Surges  
AIR ENTRAINMENT AND RELEASE  
FOR INFLOW OF 0.03 CFS



A. Air trapped in separation zone of elbow  
Photo PX-D-60626.

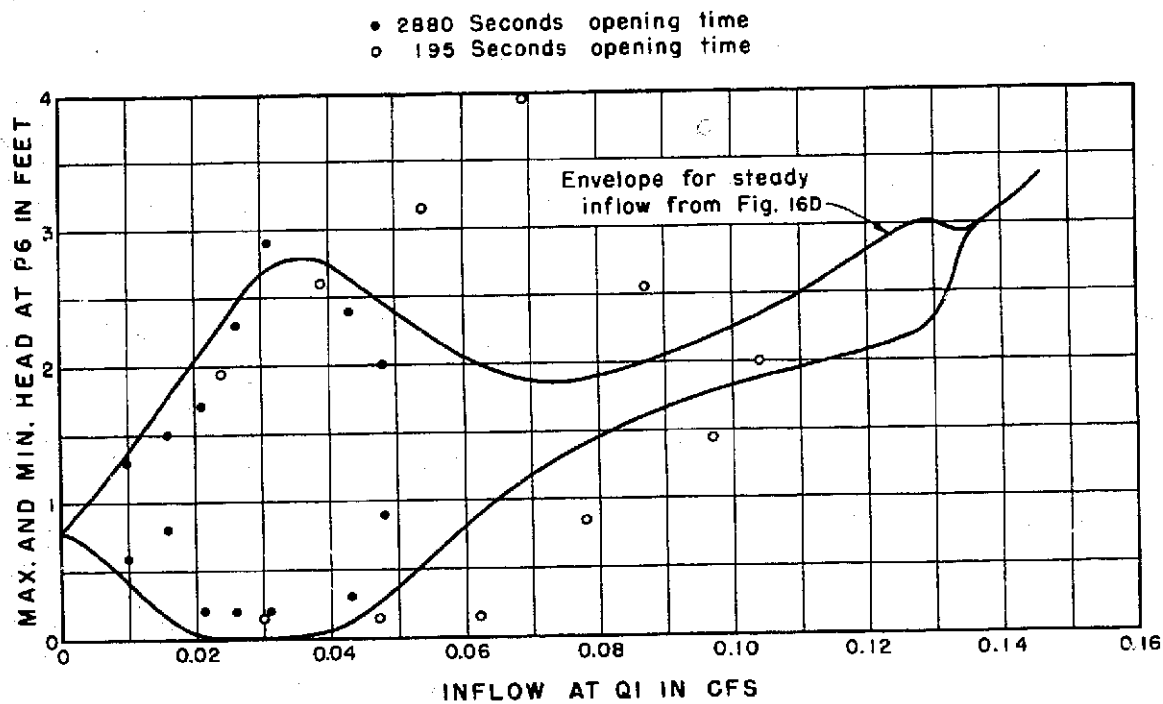


B. Air bubble rising against flow in  
downstream leg of pipe check  
Photo PX-D-60627.

Pipe Line Surges

AIR ENTRAPMENT AND RELEASE

FOR INFLOW OF 0.13 CFS



PIPE LINE SURGES  
 COMPARISON OF HEAD SURGES AT P6  
 FOR STEADY AND UNSTEADY INFLOWS  
 WITH HIGH HEAD LOSS AND WITHOUT SURGE TANK

CONVERSION FACTORS--BRITISH TO METRIC UNITS OF MEASUREMENT

The following conversion factors adopted by the Bureau of Reclamation are those published by the American Society for Testing and Materials (ASTM Metric Practice Guide, January 1964) except that additional factors (\*) commonly used in the Bureau have been added. Further discussion of definitions of quantities and units is given on pages 10-11 of the ASTM Metric Practice Guide.

The metric units and conversion factors adopted by the ASTM are based on the "International System of Units" (designated SI for Systeme International d'Unites), fixed by the International Committee for Weights and Measures; this system is also known as the Giorgi or MKSA (meter-kilogram (mass)-second-ampere) system. This system has been adopted by the International Organization for Standardization in ISO Recommendation R-31.

The metric technical unit of force is the kilogram-force; this is the force which, when applied to a body having a mass of 1 kg, gives it an acceleration of 9.80665 m/sec/sec, the standard acceleration of free fall toward the earth's center for sea level at 45 deg latitude. The metric unit of force in SI units is the newton (N), which is defined as that force which, when applied to a body having a mass of 1 kg, gives it an acceleration of 1 m/sec/sec. These units must be distinguished from the (inconstant) local weight of a body having a mass of 1 kg; that is, the weight of a body is that force with which a body is attracted to the earth and is equal to the mass of a body multiplied by the acceleration due to gravity. However, because it is general practice to use "pound" rather than the technically correct term "pound-force," the term "kilogram" (or derived mass unit) has been used in this guide instead of "kilogram-force" in expressing the conversion factors for forces. The newton unit of force will find increasing use, and is essential in SI units.

Table I

QUANTITIES AND UNITS OF SPACE

Multiply	By	To obtain
<b>LENGTH</b>		
Mil. . . . .	25.4 (exactly)	Micron
Inches . . . . .	25.4 (exactly)	Millimeters
	2.54 (exactly)*	Centimeters
Feet . . . . .	30.48 (exactly)	Centimeters
	0.3048 (exactly)*	Meters
	0.003048 (exactly)*	Kilometers
Yards . . . . .	0.9144 (exactly)	Meters
Miles (statute) . . . . .	1,609.344 (exactly)*	Meters
	1.609344 (exactly)	Kilometers
<b>AREA</b>		
Square inches . . . . .	6.4516 (exactly)	Square centimeters
Square feet . . . . .	929.03*	Square centimeters
	0.092903	Square meters
Square yards . . . . .	0.836127	Square meters
Acres . . . . .	0.40469*	Hectares
	4,046.9*	Square meters
	0.0040469*	Square kilometers
Square miles . . . . .	2.58999	Square kilometers
<b>VOLUME</b>		
Cubic inches . . . . .	16.3871	Cubic centimeters
Cubic feet . . . . .	0.0283168	Cubic meters
Cubic yards . . . . .	0.764555	Cubic meters
<b>CAPACITY</b>		
Fluid ounces (U.S.) . . . . .	29.5737	Cubic centimeters
	29.5729	Milliliters
Liquid pints (U.S.) . . . . .	0.473179	Cubic decimeters
	0.473168	Liters
Quarts (U.S.) . . . . .	946.358*	Cubic centimeters
	0.946331*	Liters
Gallons (U.S.) . . . . .	3,785.43*	Cubic centimeters
	3.78543	Cubic decimeters
	3.78533	Liters
	0.00378543*	Cubic meters
Gallons (U.K.) . . . . .	4.54609	Cubic decimeters
	4.54696	Liters
Cubic feet . . . . .	28.3160	Liters
Cubic yards . . . . .	764.55*	Liters
Acres-feet . . . . .	1,233.5*	Cubic meters
	1,233,500*	Liters

Table II  
QUANTITIES AND UNITS OF MECHANICS

Multiply	By	To obtain
<b>MASS</b>		
Grains (1/7,000 lb)	84,79891 (exactly)	Milligrams
Troy ounces (480 grains)	31,1035	Grams
Ounces (avdp)	28,3495	Kilograms
Pounds (avdp)	0,45359237 (exactly)	Kilograms
Short tons (2,000 lb)	0,907185	Metric tons
Long tons (2,240 lb)	1,016,05	Kilograms
<b>FORCE/AREA</b>		
Pounds per square inch	0,070307	Kilograms per square centimeter
Pounds per square foot	0,689476	Newtons per square centimeter
Pounds per square inch	4,88243	Kilograms per square meter
Pounds per square foot	47,8803	Newtons per square meter
<b>MASS/VOLUME (DENSITY)</b>		
Ounces per cubic inch	1,72909	Grams per cubic centimeter
Pounds per cubic foot	48,0155	Kilograms per cubic meter
Tons (long) per cubic yard	0,0160185	Grams per cubic centimeter
Tons (long) per cubic yard	1,32694	Grams per cubic centimeter
<b>MASS/CAPACITY</b>		
Ounces per gallon (U.S.)	7,4883	Grams per liter
Ounces per gallon (U.K.)	6,2362	Grams per liter
Pounds per gallon (U.S.)	119,829	Grams per liter
Pounds per gallon (U.K.)	99,779	Grams per liter
<b>BENDING MOMENT OR TORQUE</b>		
Inch-pounds	0,011591	Meter-kilograms
Foot-pounds	1,32885 x 10 <sup>8</sup>	Centimeter-dynes
Foot-pounds	1,32825	Meter-kilogram
Foot-pounds per inch	1,36592 x 10 <sup>7</sup>	Centimeter-dynas
Ounce-inches	6,4431	Centimeter-kilograms per centimeter
Ounce-inches	72,028	Gram-centimeters
<b>VELOCITY</b>		
Feet per second	30,48 (exactly)	Centimeters per second
Feet per year	0,3048 (exactly)	Meters per second
Miles per hour	0,44704 (exactly)	Kilometers per hour
Miles per hour	0,44704 (exactly)	Meters per second
<b>ACCELERATION*</b>		
Feet per second <sup>2</sup>	0,3048*	Meters per second <sup>2</sup>
<b>FLOW</b>		
Cubic feet per second (second-foot)	0,028317*	Cubic meters per second
Cubic feet per minute	0,4719	Liters per second
GALLONS (U.S.) per minute	0,06309	Liters per second
<b>FORCE*</b>		
Pounds	0,453592*	Kilograms
Pounds	4,4482*	Newtons
Pounds	4,4482 x 10 <sup>-6</sup> *	Dynes

Multiply	By	To obtain
<b>WORK AND ENERGY*</b>		
British thermal units (Btu)	0,252*	Kilogram calories
Btu per pound	1,055,06	Joules
Foot-pounds	2,323 (exactly)	Joules per gram
Foot-pounds	1,35582*	Joules
<b>POWER</b>		
Horsepower	745,700	Watts
Foot-pounds per second	0,226071	Watts
Foot-pounds per second	1,35582	Watts
<b>HEAT TRANSFER</b>		
Btu in./hr ft <sup>2</sup> deg F (k, thermal conductivity)	1,443	Milliwatts/cm deg C
Btu ft./hr ft <sup>2</sup> deg F (C, thermal conductance)	0,1240	Kg cal/hr m deg C
Btu ft./hr ft <sup>2</sup> deg F (C, thermal conductance)	1,4880*	Kg cal m/hr m <sup>2</sup> deg C
Deg F hr ft <sup>2</sup> /Btu (R, thermal resistance)	0,688	Milliwatts/cm <sup>2</sup> deg C
Btu/hr deg F (c, heat capacity)	1,781	Deg C cm <sup>2</sup> /milliwatt
Btu/hr deg F (c, heat capacity)	4,1868	J/g deg C
Btu/hr deg F (c, heat capacity)	1,040*	Cal/gram deg C
Ft <sup>2</sup> /hr (thermal diffusivity)	0,25290*	cm <sup>2</sup> /sec
Ft <sup>2</sup> /hr (thermal diffusivity)	0,02290*	m <sup>2</sup> /hr
<b>WATER VAPOR TRANSMISSION</b>		
Grains/hr ft <sup>2</sup> (water vapor transmission)	16,7	Grams/24 hr m <sup>2</sup>
Perms (permeance)	0,659	Metric perms
Perms-inches (permeability)	1,87	Metric perm-centimeters
<b>OTHER QUANTITIES AND UNITS</b>		
Multiply		
Cubic feet per square foot per day (seepage)	304,8*	Liters per square meter per day
Pounds per square foot (viscosity)	4,8824*	Kilogram second per square meter
Square feet per second (viscosity)	0,022903*	Square meters per second
Fahrenheit degrees (change)*	5/9 exactly	Celsius or Kelvin degrees (change)*
Volts per mill.	0,033337	Kilovolts per millimeter
Lumens per square foot (foot-candles)	10,764	Lumens per square meter
Ohm-circular mils per foot	0,01882	Ohm-square millimeters per meter
Milliamps per cubic foot	36,3187*	Milliamps per cubic meter
Milliamps per square foot	10,763910*	Milliamps per square meter
Gallons per square yard	4,17553*	Liters per square meter
Pounds per inch	0,13558*	Kilograms per centimeter

#### ABSTRACT

Surges of head and discharge were studied experimentally in a laboratory pipe system having check structures spaced equally along the pipe. Surges developed when the downstream portion of the check structures did not flow full. The surges were initiated by the release of air entrained in the downstream leg of the check structures, and the surges were amplified as the flow passed through the successive pipe reaches. The experiments were made for various inflows steady at the upstream end of the system. Plots of surge magnitude vs. inflow rate showed two peaks. One peak apparently resulted from surges initiated by air release through the vent downstream of the check structures; the other peak originated from surges initiated by air release through the downstream leg of the check structure. The nonlinear momentum equation was integrated numerically to predict the growth of the discharge surge from one pipe reach to the next. The results were in good agreement with the experiments for different head loss conditions and for pipe reaches with and without surge tanks.

#### ABSTRACT

Surges of head and discharge were studied experimentally in a laboratory pipe system having check structures spaced equally along the pipe. Surges developed when the downstream portion of the check structures did not flow full. The surges were initiated by the release of air entrained in the downstream leg of the check structures, and the surges were amplified as the flow passed through the successive pipe reaches. The experiments were made for various inflows steady at the upstream end of the system. Plots of surge magnitude vs. inflow rate showed two peaks. One peak apparently resulted from surges initiated by air release through the vent downstream of the check structures; the other peak originated from surges initiated by air release through the downstream leg of the check structure. The nonlinear momentum equation was integrated numerically to predict the growth of the discharge surge from one pipe reach to the next. The results were in good agreement with the experiments for different head loss conditions and for pipe reaches with and without surge tanks.

#### ABSTRACT

Surges of head and discharge were studied experimentally in a laboratory pipe system having check structures spaced equally along the pipe. Surges developed when the downstream portion of the check structures did not flow full. The surges were initiated by the release of air entrained in the downstream leg of the check structures, and the surges were amplified as the flow passed through the successive pipe reaches. The experiments were made for various inflows steady at the upstream end of the system. Plots of surge magnitude vs. inflow rate showed two peaks. One peak apparently resulted from surges initiated by air release through the vent downstream of the check structures; the other peak originated from surges initiated by air release through the downstream leg of the check structure. The nonlinear momentum equation was integrated numerically to predict the growth of the discharge surge from one pipe reach to the next. The results were in good agreement with the experiments for different head loss conditions and for pipe reaches with and without surge tanks.

#### ABSTRACT

Surges of head and discharge were studied experimentally in a laboratory pipe system having check structures spaced equally along the pipe. Surges developed when the downstream portion of the check structures did not flow full. The surges were initiated by the release of air entrained in the downstream leg of the check structures, and the surges were amplified as the flow passed through the successive pipe reaches. The experiments were made for various inflows steady at the upstream end of the system. Plots of surge magnitude vs. inflow rate showed two peaks. One peak apparently resulted from surges initiated by air release through the vent downstream of the check structures; the other peak originated from surges initiated by air release through the downstream leg of the check structure. The nonlinear momentum equation was integrated numerically to predict the growth of the discharge surge from one pipe reach to the next. The results were in good agreement with the experiments for different head loss conditions and for pipe reaches with and without surge tanks.

Holley, E R

SURGING IN A LABORATORY PIPELINE WITH STEADY INFLOW

USBR Lab Rept Hyd-580, Hyd Br, Sept 1967. Bureau of Reclamation,

Denver, Colo, 20 p, 20 fig, 3 tab, 7 ref, append

DESCRIPTORS-- \*pipelines/ \*surges/ hydraulic models/ laboratory tests/  
surge tanks/ closed conduit flow/ fluid flow/ fluid mechanics/ computer  
programming/ hydraulics/ air entrainment/ check structures/ oscillation/  
\*water pipes/ momentum

IDENTIFIERS-- \*pipeline surges/ Runge-Kutta method/ surge waves

Holley, E R

SURGING IN A LABORATORY PIPELINE WITH STEADY INFLOW

USBR Lab Rept Hyd-580, Hyd Br, Sept 1967. Bureau of Reclamation,

Denver, Colo, 20 p, 20 fig, 3 tab, 7 ref, append

DESCRIPTORS-- \*pipelines/ \*surges/ hydraulic models/ laboratory tests/  
surge tanks/ closed conduit flow/ fluid flow/ fluid mechanics/ computer  
programming/ hydraulics/ air entrainment/ check structures/ oscillation/  
\*water pipes/ momentum

IDENTIFIERS-- \*pipeline surges/ Runge-Kutta method/ surge waves

Holley, E R

SURGING IN A LABORATORY PIPELINE WITH STEADY INFLOW

USBR Lab Rept Hyd-580, Hyd Br, Sept 1967. Bureau of Reclamation,

Denver, Colo, 20 p, 20 fig, 3 tab, 7 ref, append

DESCRIPTORS-- \*pipelines/ \*surges/ hydraulic models/ laboratory tests/  
surge tanks/ closed conduit flow/ fluid flow/ fluid mechanics/ computer  
programming/ hydraulics/ air entrainment/ check structures/ oscillation/  
\*water pipes/ momentum

IDENTIFIERS-- \*pipeline surges/ Runge-Kutta method/ surge waves

Holley, E R

SURGING IN A LABORATORY PIPELINE WITH STEADY INFLOW

USBR Lab Rept Hyd-580, Hyd Br, Sept 1967. Bureau of Reclamation,

Denver, Colo, 20 p, 20 fig, 3 tab, 7 ref, append

DESCRIPTORS-- \*pipelines/ \*surges/ hydraulic models/ laboratory tests/  
surge tanks/ closed conduit flow/ fluid flow/ fluid mechanics/ computer  
programming/ hydraulics/ air entrainment/ check structures/ oscillation/  
\*water pipes/ momentum

IDENTIFIERS-- \*pipeline surges/ Runge-Kutta method/ surge waves